

## Abstract

Atmospheric blocking disturbs synoptic scale features from normal eastward progression, creating anomalous atmospheric conditions for the duration of the blocking event, during which the likelihood of extreme weather events is enhanced. The essence of blocking can be captured through identifying periods of large scale, long lasting height anomalies at the 500-hPa level.

Using NCEP-NCAR Reanalysis V2 data (JFM) 1980-2016, long lasting (greater than 8 consecutive days) blocking events are classified by applying the threshold crossing method (Dole and Gordon 1983) to daily average 500-hPa geopotential height field anomalies at a key point in the North Atlantic. A composite of the 30 cases identified reveals a blocking precursor signal in the Pacific in approximately 2 weeks before the onset of the North Atlantic blocking event.

Identifying Precursors to Winter Time Atlantic Blocking Events

Greg Porter

A scholarly paper in partial fulfillment of the requirements for the degree of Master of Science  
April 2017

Department of Atmospheric and Oceanic Sciences

University of Maryland

College Park, Maryland

Advisor: Dr. Daryl Kleist

# Table of Contents

|   |           |
|---|-----------|
| <b>ACKNOWLEDGEMENTS</b> .....                     | <b>4</b>  |
| <b>LIST OF FIGURES</b> .....                      | <b>5</b>  |
| <b>LIST OF SYMBOLS</b> .....                      | <b>7</b>  |
| <br>  |           |
| <b>CHAPTER 1: LITERATURE REVIEW</b> .....         | <b>8</b>  |
| 1.1 INTRODUCTION TO ATMOSPHERIC BLOCKING .....    | 8         |
| 1.2 DYNAMICS OF ATMOSPHERIC BLOCKING .....        | 10        |
| 1.2.1 STATIONARY WAVES.....                       | 11        |
| 1.2.2 TROPICAL FORCING.....                       | 12        |
| 1.2.3 BARATROPIC INSTABILITIES .....              | 13        |
| 1.2.4 TRANSIENT EDDIES AND LARGE SCALE FLOW ..... | 13        |
| 1.3 SUMMARY .....                                 | 16        |
| <br>  |           |
| <b>CHAPTER 2: RESULTS AND METHODOLOGY</b> .....   | <b>17</b> |
| 2.1 DATASET .....                                 | 17        |
| 2.2 BLOCKING REGIME IDENTIFICATION .....          | 18        |
| 2.3 COMPOSITES .....                              | 20        |
| <br>  |           |
| <b>CHAPTER 3: RESULTS AND DISCUSSION</b> .....    | <b>22</b> |
| 3.1 COMPOSITE STRUCTURE FOR DURATION .....        | 22        |
| 3.1.1 500-hPa GEOPOTENTIAL HEIGHT ANOMALIES ..... | 22        |
| 3.1.2 TROPOSPHERIC WIND ANOMALIES .....           | 24        |
| 3.2 LAGGED COMPOSITES AND EVOLUTION .....         | 28        |
| 3.2.1 FIFTEEN TO TWENTY DAYS PRIOR TO ONSET.....  | 29        |
| 3.2.2 TEN TO FIFTEEN DAYS PRIOR TO ONSET.....     | 29        |
| 3.2.3 FIVE TO TEN DAYS PRIOR TO ONSET .....       | 31        |
| 3.2.4 ZERO TO FIVE DAYS PRIOR TO ONSET.....       | 33        |
| 3.3 HOVMÖLLER DIAGRAM OF PRECURSORS.....          | 36        |
| 3.4 NA BLOCKING AND TELECONNECTIONS .....         | 36        |
| <br>  |           |
| <b>CHAPTER 4: SUMMARY AND FUTURE WORK</b> .....   | <b>41</b> |
| <b>REFERENCES</b> .....                           | <b>43</b> |
| <b>SUPPLEMENTARY FIGURES</b> .....                | <b>46</b> |

## Acknowledgements

Where do I begin! So many people have been instrumental in not only my completion of this Master of Science degree, but in my entire academic journey and life. My sincere thanks to the following:

To my late grandfather, whose, unbeknownst to him, simple and holistic weather observations fueled my passion to become an atmospheric scientist. To my siblings Andy, Michelle, Kelly and their spouses for their continued interest and support in my career and academic progress, even if it came in the form of a “how much snow are we going to get?” text every now and again! And to their little ones, my nieces and nephew, for allowing me to express my inner child like self and be a goofy “Uncle Duck”. To friends from all walks of life; Boston, UMass Lowell and the University of Maryland for keeping me grounded and level headed.

To Maggie, I cannot even begin to quantify how much you’ve meant to me during this entire process. I came to this University only seeking a degree, but what I found something infinitely more valuable in you. Mags, you are my best friend, the love of my life and my puzzle piece and I would not have been able to finish without you.

Last, but most certainly not least, to my parents Andy and Marie. For so many things it would require an additional 50 pages of text! But ultimately, for always and unconditionally believing in me and never letting me give up. This paper and degree, above anything else, is a testament to 33 years of your love and support.

## List of Figures

|  |    |
|--|----|
| <b>Figure 1:</b> Illustration of Rex and Omega block .....   | 9  |
| <b>Figure 2:</b> Annual climatological location frequency for atmospheric blocks and boreal winter climatological locations for standing waves at the surface..... | 12 |
| <b>Figure 3:</b> Schematic of eddy straining (Shutts, 1983) .....  | 14 |
| <b>Figure 4:</b> North Atlantic key region.....  | 18 |
| <b>Figure 5:</b> Blocking frequency (Pelly and Hoskins, 2003).....   | 19 |
| <b>Figure 6:</b> Dates and duration of 30 NA blocking events .....   | 21 |
| <b>Figure 7:</b> 5-day average composite SLP 10 to 15 days prior to blocking onset .....   | 22 |
| <b>Figure 8:</b> Composited 500-hpa height anomalies for duration .....  | 23 |
| <b>Figure 9:</b> Composited precipitation anomalies for duration .....   | 25 |
| <b>Figure 10:</b> Composited mean vector wind anomalies for duration .....   | 26 |
| <b>Figure 11:</b> Composited u-wind anomalies for duration .....   | 27 |
| <b>Figure 12:</b> Composited v-wind anomalies for duration .....   | 28 |
| <b>Figure 13:</b> 5-day averaged composited anomalies 15 to 20 days prior to blocking onset .....  | 30 |
| <b>Figure 14:</b> 5-day averaged composited anomalies 10 to 15 days prior to blocking onset .....  | 32 |
| <b>Figure 15:</b> 5-day average composited anomalies 5 to 10 days prior to blocking onset .....  | 34 |
| <b>Figure 16:</b> 5-day average composited anomalies 0 to 5 days prior to blocking onset.....  | 35 |
| <b>Figure 17:</b> Hovmöller diagram of v-wind anomalies for duration.....  | 37 |
| <b>Figure 18:</b> Winter Height anomalies associated with the positive phase of the a.) PNA, b.) NAO and the negative phase of the AO.....                         | 38 |

**Figure 19:** Winter height anomalies for positive phase of PNA compared to height anomalies for duration of NA blocking events.....39

**Figure 20:** Composited PNA, NAO and AO indices leading up to NA blocking onset.....40

### **Supplemental Figures**

**Figure 21:** Frequency distribution of NA blocking events.....46

**Figure 22:** Total number of NA blocked events vs blocked days.....47

**Figure 23:** Climatology of winter time 500-hPa heights from 1980-2016.....48

**Figure 24:** 5-day averaged composite anomalies for 500-hPa heights, v-wind and u-wind anomalies 0-5 days after blocking onset.....49

**Figure 25:** Diagram of flow anomalies associated with highly amplified jet.....50

**Figure 26:** Hovmoller diagram of v-wind anomalies for one NA blocking event.....51

## List of Symbols

**netCDF**- Network Common Data Form file

**hPa** – Hectopascal

**NA blocking event** – One of the 30 identified North Atlantic blocking events from this study

**SST** – Sea Surface Temperature

**NAO** – North Atlantic Oscillation

**RWB** – Rossby Wave Breaking

**PNA** – Pacific North American Oscillation

**AO** – Arctic Oscillation

# Chapter1: Literature Review

## 1.1 Introduction to Atmospheric Blocking

Mid-latitude climate is characterized by strong westerly winds called jet streams. Typically, jet streams are located somewhere between 30°N-40°N. During winter, planetary waves can break the “equilibrium” state defined by the consistent presence of jet streams. This leads to circulation anomalies often characterized by a strong meridional component. Atmospheric blocking can be thought of as an event associated with this circulation anomaly, that is, a high-pressure system characterized by anti-cyclonic flow that blocks or diverts the normally westerly flowing jet.

Atmospheric blocking events and the weather anomalies associated with them have been observed as early as the early 20<sup>th</sup> century. However, a true scientific investigation and classification of blocking characteristics was not completed until the middle of the 20<sup>th</sup> century. Namias (1947) first described atmospheric blocking as a weather pattern associated with a reduction in zonal flow. A few years later, Elliott and Smith (1949) noted a strong meridional anomaly associated with blocking events, one that caused the “obstruction of the normal eastward progress of migratory cyclones”. That same year, Berggren (1949) used upper air observations to monitor the development of planetary waves during blocking events, ultimately resulting in a split jet stream.

The first formal definition for atmospheric blocking came from Rex (1950 a, b), where he defined blocking as a “quasi-stationary, long-lasting, barotropic weather system that modifies westerly flow and blocks the eastward movement of migratory cyclones”. Rex noted that during blocking events, the atmosphere transferred from a “high energy state” (strong zonal flow) to a “low energy state” (strong meridional flow). This low energy state features a “train of cyclonic



and anti-cyclonic vortices”, whereby the main feature of a blocking event was the presence of a “quasi-stationary warm ridge or anti-cyclone just downstream from the breakdown of westerly flow”. Rex also provided the first spatial and temporal definitions for blocking events, with the original blocking definition requiring at least a 10-day persistent anomaly spread out zonally over at least 45°. With a proper definition for atmospheric blocking, Rex then went on to describe the temperature and precipitation anomalies associated with blocking events as well as the prevalence for blocking to develop in the eastern Atlantic and Pacific basins.

The first classification of different categories of blocking was completed by Sumner (1954). A Rex or diffluent block (Figure 1) is classified by a meridionally oriented dipole of high pressure and low pressure. The second classification (Figure 1) is called an omega block, so named for its resemblance to the Greek letter  $\Omega$ . An omega block is defined as a large high pressure system with two low pressure systems located upstream and downstream of the central high pressure.

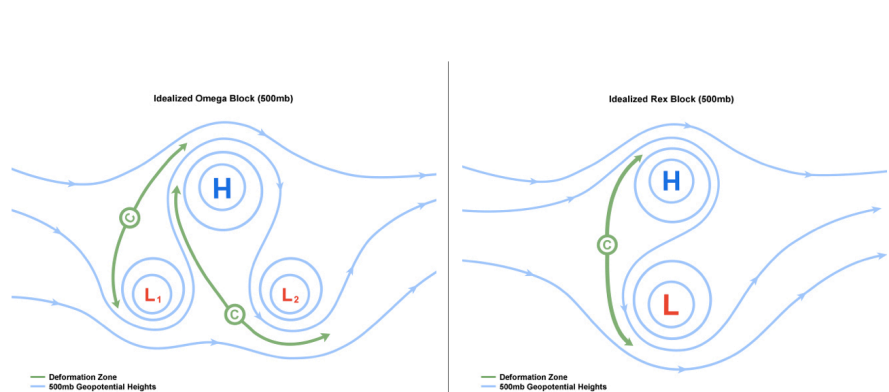


**Figure 1:** Illustration of an Omega block (left) and a Rex block (right). The green arrows represent the stretching caused by deformation. Notice the enhanced meridional stretching associated with both block types. Via UCAR [http://www.meted.ucar.edu/norlat/sat\\_features/blocking\\_patterns/index.htm](http://www.meted.ucar.edu/norlat/sat_features/blocking_patterns/index.htm)

Largely based on these original classifications, several studies in the late 20<sup>th</sup> century furthered the knowledge of atmospheric blocking as a phenomenon through the creation of climatologies (Dole and Gordon, 1983; Tibaldi and Molteni, 1990). From these climatologies, the classification of atmospheric blocking generally fell into two groups. The first classified a blocking event whereby anomalies must persist for at least 5 days and extend across at least 10° latitude (Tibaldi and Molteni, 1990; Pelly and Hoskins, 2003; Barriopedro, 2006). The second method, employed by this study, defines blocking through persistent anomalies of geopotential height or potential vorticity (Dole and Gordon, 1983; Schwierz et al., 2004).

As noted in section 1.1, anomalous weather conditions associated with atmospheric blocking were recognized since the early 20<sup>th</sup> century. Recently, several studies investigated the link between extreme weather and blocking more thoroughly (Green, 1977; Trigo et al., 2004; Stillmann et al., 2011). Such studies showed that large scale subsidence associated with blocking highs can lead to prolonged heat waves and drought. Flow anomalies created by blocking events also create extreme conditions downstream as well. For example, winter time Arctic outbreaks in the mid-latitudes are often the result of persistent anti-cyclonic flow bringing cold air in from higher latitudes.

## **1.2 Dynamics of Atmospheric Blocking**

Despite several decades of research on atmospheric blocking, the scientific community has never come to a full consensus as to the dynamics and driving forces behind the phenomenon. Rossby (1950) and Rex (1950a) provided the first attempt at a physical explanation, comparing the jet stream to a hydraulic jump whereby the jet stream acts as a conduit that breaks down a high kinetic energy jet upstream to a low kinetic energy jet downstream.

Improved modeling and computational power allowed for more rigorous testing of dynamical theories over the next several decades. Advanced computing enabled researchers to approach the problem from a mathematical framework using the governing atmospheric equations. Combining the mathematics with the physics of atmospheric blocking resulted in several accepted theories.

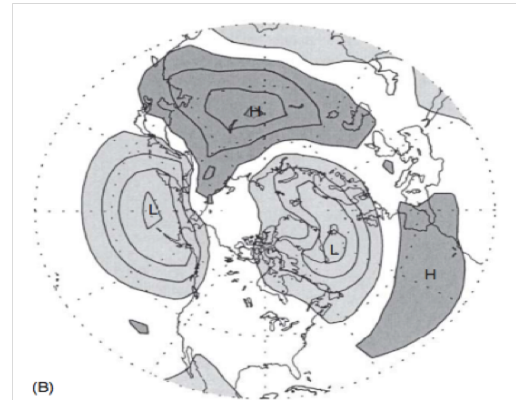
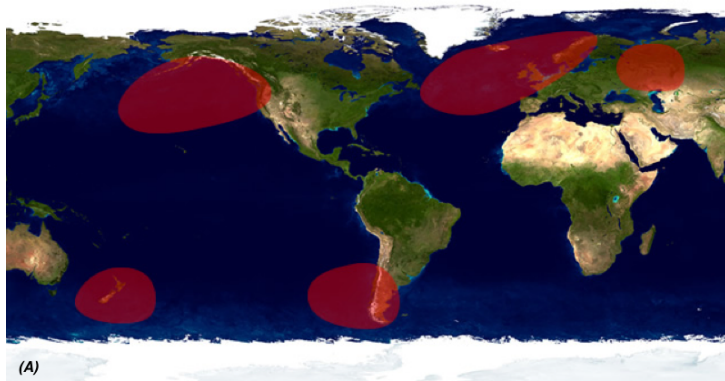
### ***1.2.1 Stationary Waves***

Figure 2 shows the annual climatological location of atmospheric blocks as well as the winter time average location of stationary waves. Stationary waves form because of topography and temperature differences that arise from land/sea contrasts. They manifest themselves as long lasting surface pressure anomalies that persist for months at a time (Held et al., 2002).

Simple visual analysis of both images (Figure 2) suggests a tendency for the average position of blocks to overlap with the average position of stationary waves. Therefore, it stands to reason that atmospheric blocking may be connected to large scale flow driven by thermal contrasts or continental elevation (Grose and Hoskins, 1979).

Given the possible connection to large scale flow, other studies investigated the link between transient Rossby waves and their linear interactions (Tung and Lizden, 1979) and non-linear interactions (Egger, 1978) with standing waves. The interaction between transient eddies and standing waves will serve as an important dynamical precursor for the blocking events used in this study.

### Climatological Locations of Blocks



**Figure 2:** A.) Annual climatological location frequency for atmospheric blocks (From UCAR [http://www.meted.ucar.edu/norlat/sat\\_features/blocking\\_patterns/overview.htm](http://www.meted.ucar.edu/norlat/sat_features/blocking_patterns/overview.htm)). B.) Boreal winter climatological locations for standing waves at the surface. L represents low pressure and H represents high pressure. (From Nigam and DeWeaver 2003 <http://www.atmos.umd.edu/~nigam/Encyc.Atmos.Sci.Stationary.Waves.Nigam-DeWeaver.2003.pdf>)

### 1.2.2 Tropical Forcing

Forcing from tropical anomalies on mid-latitude weather was first identified by Hoskins and Karoly (1981). Using a linearized baroclinic model, they showed a significant atmospheric response in the mid-latitudes could be obtained through simple forcing at tropical latitudes. The forcing in the mid-latitudes was represented in the upper levels in the form of Rossby wave train, with longer waves propagating poleward and shorter waves becoming trapped south of the mid-latitude jet stream. The out of phase signal from the two wave trains resulted in the development of a block like structure.

Recent studies of tropical forcing confirmed Hoskins and Karoly's results, concluding that a similar wave train like response in the mid-latitude upper atmosphere. Cassou (2008) showed that Madden-Julian-Oscillation phases could excite a series of upper level wave trains that could affect weather in the North Atlantic. Hoskins and Sardenshmukh (1987) and Ferranti

et al. (1994) showed that blocking frequency in the North Atlantic varied with SST anomalies over Indonesia and the Caribbean Sea.

### ***1.2.3 Barotropic Instabilities***

Some studies have suggested a dynamical importance between barotropic instability and maintenance of an atmospheric blocking event once it has developed. Barotropic disturbances derive their energy from the mean flow, where energy considerations show that for a barotropic disturbance to grow, it must tilt in the opposite direction of the zonal flow. In general, mid-latitude disturbances tilt in the same direction as the zonal flow, making barotropic instability a poor method of intensification. However, mid-latitude disturbances like atmospheric blocks decay because of barotropic instability, where the disturbance gives up some of its energy to the mean flow. Studies from Frederiksen (1997) and Simmons et al. (1983) investigated recurring patterns like the frequent blocking patterns found in the eastern Pacific and eastern Atlantic (Figure 2). These studies showed that after the onset of atmospheric blocking, the fastest growing modes derived their energy from the basic atmospheric state through barotropic instabilities. These results suggest that barotropic instabilities may play an important role in the persistence of atmospheric blocking events.

### ***1.2.4 Transient Eddies and Large Scale Flow***

Synoptic scale or transient eddies represent the most accepted theory of a forcing mechanism for the onset and maintenance of atmospheric blocks. First purposed by Berggren et al. (1949), he observed that small synoptic disturbances approaching a blocking ridge would

undergo a “distinct shrinking in the meridional direction”, ultimately forming both cyclonic and anti-cyclonic eddies that became absorbed by the block.

The first physical pathway to the synoptic eddy forcing theory was provided by Shutts (1983). In this study, Shutts introduced the concept of eddy straining (Figure 3), whereby eddies propagated along a distinct baroclinic zone (i.e. jet stream) when they encounter a blocking ridge of high pressure, becoming stretched in the meridional direction. As these eddies become embedded within the block, they transfer energy progressively at low wavenumbers. An example of such a transfer is a synoptic scale eddy providing vorticity to a block. Physically speaking, the vorticity forcing provided by the synoptic scale eddy would prevent the block “from being blown away by the mean flow rather than against friction” (Shutts, 1983).

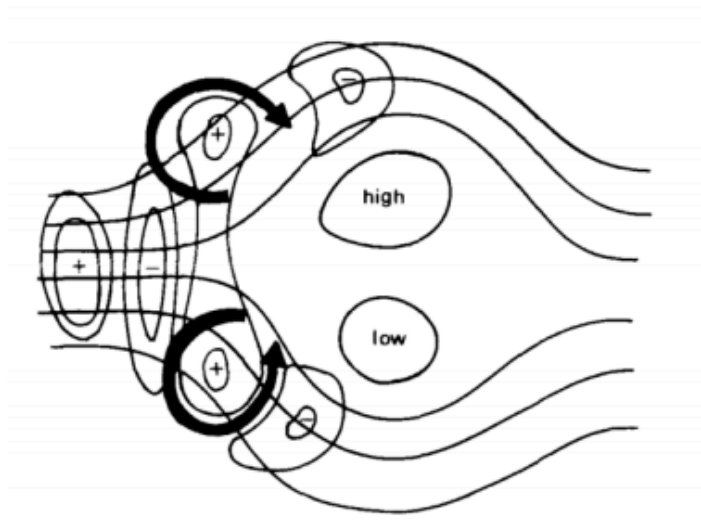


**Figure 3:** Schematic representation of eddy straining. As transient eddies approach the split jet (anti-cyclone), they become elongated in the meridional direction, transferring vorticity (black arrows) to the large-scale anomaly. From Shutts (1983)

Through the introduction of eddy straining as a forcing mechanism, Shutts showed that blocking can arise naturally, even in the absence of orography. Such a conclusion suggests that transient eddies can not only maintain a block, but also initiate the onset of a block.

Other studies later reinforced Shutts' eddy straining theory. Perhaps the most important of these was published in the same year as Shutts paper. Hoskins et al. (1983) introduced the E-vector used to compute momentum transport by transient eddies, thus enabling him to show that elongation of transient eddies upstream from a block produces easterly winds downstream, reinforcing the block structure.

The interaction of strong synoptic scale eddies and the onset of blocking events has also been investigated thoroughly. Hansen and Chen (1982) studied two blocking episodes in the Atlantic and Pacific, discovering that in both cases, blocking developed downstream of intense storm activity or explosive cyclogenesis. Tsou and Smith (1990) showed that vorticity forcing associated with explosive cyclogenesis was crucial during the onset of a blocking event. Colucci and Alberta (1996) studied 7 consecutive winters to draw conclusions on the relationship between cyclogenesis and the onset of blocking. They found that cyclogenesis only has a distinct impact on the onset of blocking events when planetary waves could "precondition" the background flow through a strong positive meridional flow. Building on this study, Nakamura (1997) showed that feedbacks between eddies and synoptic perturbations were much more prevalent in the Pacific basin, while large scale anomalies from planetary waves were more common in the Atlantic. The difference likely arises from the larger displacement between the eddy driven jet and subtropical jet that occurs in the Atlantic.

With the importance of planetary wave dynamics established, studies in the early 21<sup>st</sup> century moved toward investigating atmospheric blocks through a potential vorticity framework. Pelly and Hoskins (2003) created a new blocking index by studying the dynamical tropopause response to blocking, ultimately connecting the phenomenon to Rossby wave breaking (RWB) dynamics. More recently, studies showed that Rossby wave trains over the Atlantic were

identified as a precursor to Atlantic blocking events (Woollings et al., 2008; Tyrlis and Hoskins, 2008).

Lastly, recent studies have investigated the link between atmospheric blocking and teleconnections, specifically the North Atlantic Oscillation (NAO). Benedict (2004) and Franzke et al. (2004) showed a connection between the NAO and RWB and the distinct roles that cyclonic and anti-cyclonic wave breaking have on the weather pattern.

### **1.3 Summary**

It is clear that much work has been done on the dynamics behind the onset and maintenance of atmospheric blocking. From these works, we can build a conceptual consensus to justify the investigation methods and parameters used to detect precursors to the atmospheric blocking events identified in this study.

The most accepted theory on the dynamics of atmospheric blocking involve the interaction of different components of the climate, such as orographic forced waves, thermally forced waves and the interaction of baroclinic eddies with the mean atmospheric flow. As such, a lot of importance has been placed on the RWB interpretation of atmospheric blocking and its associated atmospheric characteristics.

The remainder of this paper will seek to investigate the precursor signals that arise from the RWB dynamics associated with NA blocking events. Chapter 2 discusses the data, experiment setup and composite technique used to identify 30 blocking cases in this study. Chapter 3 presents a discussion of the dynamics of the composited NA blocking events as well as the identification of precursor signals generated by the RWB interpretation of atmospheric blocking. Chapter 3 also presents a more robust view on the rossby wave train anomalies used to



identify precursor signals for the 30 NA blocking events. Finally, chapter 4 will summarize the findings from this study and present possible pathways for future work.

## **Chapter 2: Data and Methodology**

### **2.1 Datasets**

NCEP/NCAR Reanalysis (Kalnay et al. 1996; hereafter referred to as NCEP/NCAR) mean daily 500-hPa geopotential heights in January, February and March for the 37-year period from 1980-2016 are used to identify blocking events. The NCEP dataset has a spatial coverage of 2.5-degree latitude x 2.5-degree longitude across a global grid and a vertical distribution across 17 pressure layers. Geopotential heights are computed 4 times per day at each grid point and each vertical level. The mean daily 500-hPa geopotential height is computed as an average of these 4 computations.

In addition to 500-hPa geopotential heights, the mean zonal, meridional and vector winds at 200-hPa from NCEP were used in the diagnosis of precursors to identified blocking events. Long term climatological means are based on NCEP data from 1981-2010. Anomalies of variables were calculated as departures (daily mean – monthly climatology) from the long term climatological mean.

Teleconnection data was also utilized in this experiment. Daily teleconnection data was obtained from the mean of the 11-member ERSI/PSD GEFS reforecast ensemble forecasts. 3-month seasonal averaged teleconnection data was obtained from the Climate Prediction Center seasonal mean.

## 2.2 Blocking Regime Identification

Blocking events were identified by using the threshold crossing procedure (Dole and Gordon, 1983) applied to the daily 500-hPa geopotential height anomaly field. Several studies have used a similar approach to identify blocking events (Higgins and Schubert, 1996; Renwick, 1998; Black and Evans, 1998; Schwierz et al., 2004; Carrera et al., 2004). The threshold parameters chosen for this study were 100 m and 8 days. Previous studies (Carrera et al., 2004) have the 100-m value for 500-hPa geopotential heights, while other studies (Dole and Gordon, 1983; Higgins and Schubert, 1996) have used a temporal parameter between 8 and 10 days. For this study, using the 8-day parameter provides more of an opportunity to identify blocking events. A blocked day is defined as any day in which the daily mean 500-hPa geopotential height anomaly exceeds 100-m. A blocked event is defined as a 100-m departure of the daily mean 500-hPa geopotential height for 8 consecutive days.

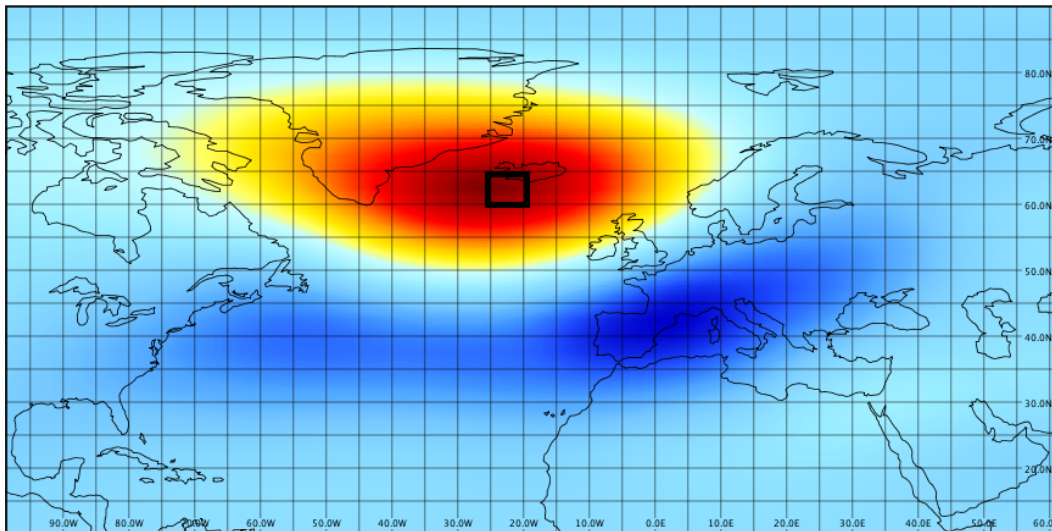


*Figure 4: Key region used in this study. The black box covers the longitude 20°W-25W and 60°N-65N.*

This study employs a “key region” (Figure 4) located within the grid box at 60N°-65°N, 20°W-25°W in the North Atlantic. In contrast to dynamic blocking identification schemes which are calculated over an entire basin, the key region was selected as a local maximum of blocking frequency in the boreal winter. Studies have shown that a peak in winter time blocking frequency occurs around the 22.5°W longitude (Pelly and Hoskins, 2003), which serves as the basis for the location of the key region in this study.

A blocked day must meet the 100-m positive geopotential height anomaly mentioned above over the entire grid box defined by the key region. A blocked event (herby referred to as an NA blocking event) must meet the geopotential height anomaly over the entire grid box for at least 8 consecutive days. The combination of the temporal and spatial restrictions used in this study ensures the rigorous identification of strong, long duration blocking events

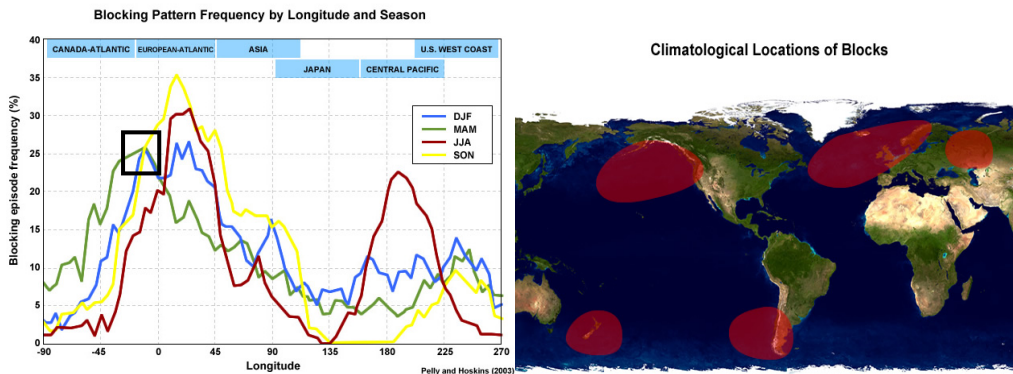


**Figure 5:** Blocking frequency distribution (on left) from Pelly and Hoskins (2003). The black box highlights the peak wintertime blocking. Seasonal climatological frequency (via UCAR [http://www.meted.ucar.edu/norlat/sat\\_features/blocking\\_patterns/overview.htm](http://www.meted.ucar.edu/norlat/sat_features/blocking_patterns/overview.htm)) of blocking events. The annual frequency of high latitudinal blocking combined with the winter time frequency near 22.5W provides the basis for the key region in this study.

Analysis of NA blocking events was restricted to onset times that fell in between the months of January through March over the 37-year period. This study's timeframe represents a slight variation from the boreal (December – February) winter timeframe to capture the tendency for a peak in blocking frequency during the early spring (Figure 5).

The blocking regime identification resulted in a total of 30 events (Figure 6). Out of the potential 3340 days, a total of 328 days or 9.8% belonged to blocking events. The blocking events ranged from 8-22 days in length with a mean length of 10.1 days. For posterity, the key region had a total of 742 days or 22.2% blocked days over the 37-year period. events ranged from 8-22 days in length with a mean length of 10.1 days. For posterity, the key region had a total of 742 days or 22.2% blocked days over the 37-year period. from 8-22 days in length with a mean length of 10.1 days. For posterity, the key region had a total of 742 days or 22.2% blocked days over the 37-year period.

## **2.3 Composites**

Composites for this study were created with the assistance of the NOAA/ERSL Physical Sciences Division ([www.ersl.noaa.gov/psd](http://www.ersl.noaa.gov/psd)). The composites were grouped by mean and anomaly. Mean composites were computed as the average of the variable over the specified dates while the anomalies were computed as the daily average's departure from climatology (Figure 7). Data was retrieved for the specified dates in netCDF format and uploaded to the NOAA/ERSL compositing software. The composited data was then used to produce plots in python. Hovmoller plots were created using the NOAA/ERSL plotting software.

| Year | Event Dates                   | Duration (Days) |
|------|-------------------------------|-----------------|
| 1983 | February 4th- February 20th   | 16              |
| 1984 | March 5th- March 17th         | 12              |
| 1985 | Jananuary 1st- January 19th   | 18              |
| 1985 | February 2nd - February 10th  | 8               |
| 1986 | February 1st- February 9th    | 8               |
| 1986 | Febraury 22nd - March 1st     | 8               |
| 1987 | January 20th -January 30th    | 10              |
| 1987 | February 14th - February 23rd | 9               |
| 1988 | February 22nd - March 4       | 12              |
| 1991 | February 5th - February 15th  | 10              |
| 1992 | January 11th - January 20th   | 9               |
| 1996 | January 24th -February 3rd    | 10              |
| 1997 | January 1st - January 11th    | 10              |
| 1998 | January 23rd -February 3rd    | 11              |
| 2000 | January 12th - January 25th   | 13              |
| 2003 | January 3rd - January 11th    | 8               |
| 2003 | March 11th - March 20th       | 9               |
| 2004 | February 21st - March 1st     | 9               |
| 2005 | January 21st - February 2nd   | 9               |
| 2005 | February 18th - March 12th    | 22              |
| 2006 | January 23rd -February 10th   | 18              |
| 2006 | February 19th - March 2nd     | 11              |
| 2007 | January 21st - January 29th   | 8               |
| 2010 | January 1st - January 12th    | 12              |
| 2010 | February 5th - February 15th  | 10              |
| 2010 | March 6th - March 16th        | 10              |
| 2012 | March 22nd - March 31st       | 8               |
| 2013 | February 21st - March 3rd     | 11              |
| 2015 | January 31st - February 9th   | 10              |
| 2016 | March 13th - March 22nd       | 9               |

*Figure 6: Dates and duration of NA blocking events*

Lagged composites were computed from the onset of each blocking event. For example, a 5-day lagged composite was created by first subtracting 5 days from each of the 30 onset dates and compositing the results.

5 Day Average SLP Anomalies  
10 to 15 days prior to onset

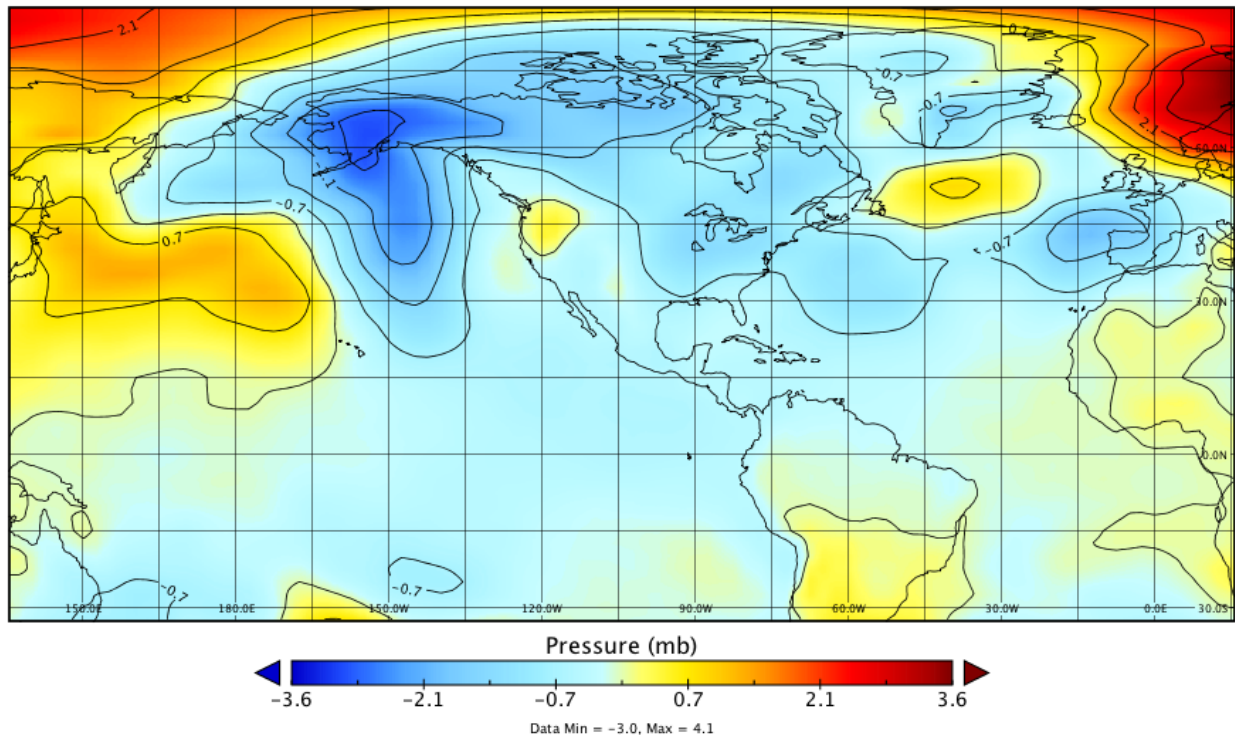


*Figure 7: 5 day averaged lagged composite of sea level pressure (SLP) for 10 to 15 days prior to NA blocking event onset*

## Chapter 3: Results

### 3.1 Composite Structure for Duration

In this section, the composite structure associated with NA blocking events is presented. The dynamics and evolution of the NA blocking events are discussed with a specific emphasis placed on circulation anomalies within 500-hPa geopotential heights and tropospheric winds.

#### 3.1.1 500-hPa Geopotential Height Anomalies

The composited 500-hPa height anomalies for the duration of all 30 blocking events are shown below (Figure 8). As mentioned in section 2.2, anomalies are calculated as the departure from the daily mean averages from (1980-2010). A strong positive height anomaly exists

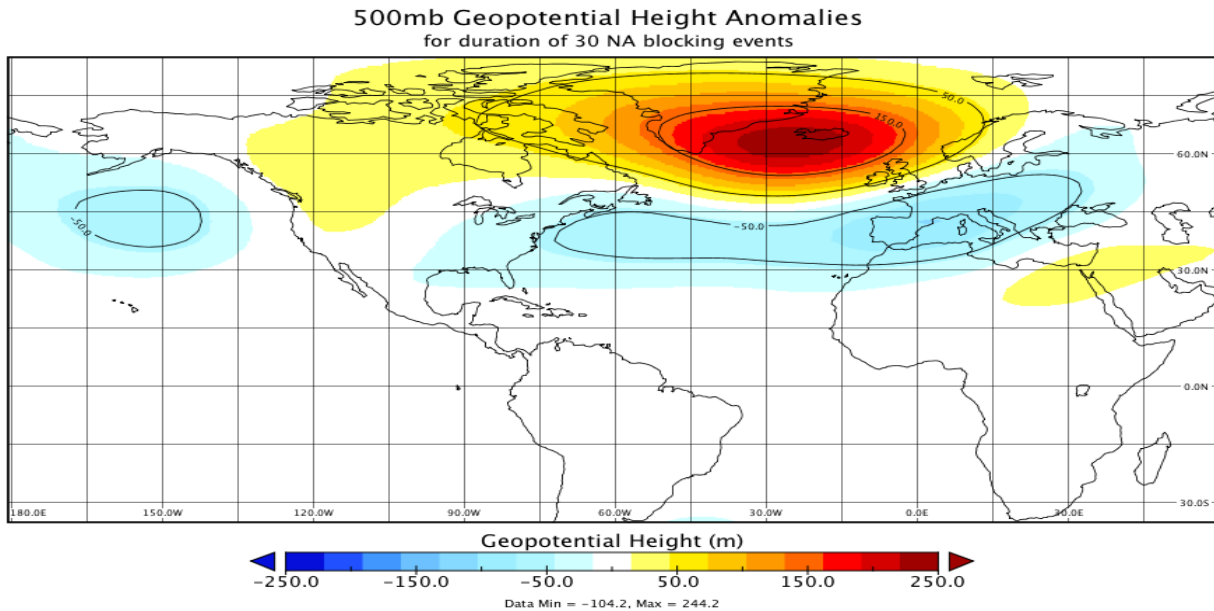


**Figure 8:** Composited 500-hPa height anomalies for the duration of all 30 NA blocking events. A strong positive height (red) anomaly exists near Iceland, while a stretch of negative height anomalies (blue) representing a displaced storm track exists to the south.

near the key region, with a maximum height anomaly peaking at more than 250 m. By itself, this result is not surprising given that the goal of this study was to isolate anomalously strong blocking events in the winter time North Atlantic.

However, the composited height anomalies displayed in Figure 8 do reveal some crucial atmospheric circulation responses in the presence of the NA blocking event. A large area of negative height anomalies stretches from the eastern United States to western Europe, spread out over the latitudes 30°N and 45°N. This area of low geopotential height anomalies represents a winter time storm track, contained to the south of the center of the blocking ridge. Similar

displacements of storm tracks (Rex, 1950; Woolings et al., 2010) either to the north or south of blocking ridges are a common atmospheric response to persistent atmospheric blocking.

A broad ridge of high pressure and associated anti-cyclonic flow dominates the western United States (U.S.). Further to the west, an upper level low (denoted by negative height anomaly) sits to the southeast of the Aleutian Islands. Figure 8 highlights the extent of the split jet stream flow both upstream and downstream of an NA blocking center.

A full investigation into the sensible weather changes related to atmospheric blocking is beyond the scope of this study. However, we can use precipitation anomalies (Figure 9) to visualize the magnitude of a surface anomaly created in the wake of an NA blocking event. A positive precipitation anomaly co-located with the negative 500-hPa height anomalies shown in Figure 8 indicates an increase in storm activity along the southerly displaced storm track. Regional anomalies are evident as well. Figure 9 shows a strong positive precipitation anomaly over southeast Greenland along with a strong negative precipitation anomaly to the west of Great Britain. These anomalies are the localized atmospheric response to persistent anti-cyclonic flow around the center of the blocking high. A similar anomalous precipitation response (Carrera et al., 2004) was shown to occur in the Pacific basin in the presence of a strong winter time Aleutian blocking high.

### ***3.1.2 Tropospheric Wind Anomalies***

Figure 10 displays the 250-hPa mean vector wind for the duration of all 30 NA blocking events. The vector wind is made up of two components, the *u-wind* (zonal) and the *v-wind*



Composited Precipitation Rate Anomalies  
for duration of 30 NA blocking events

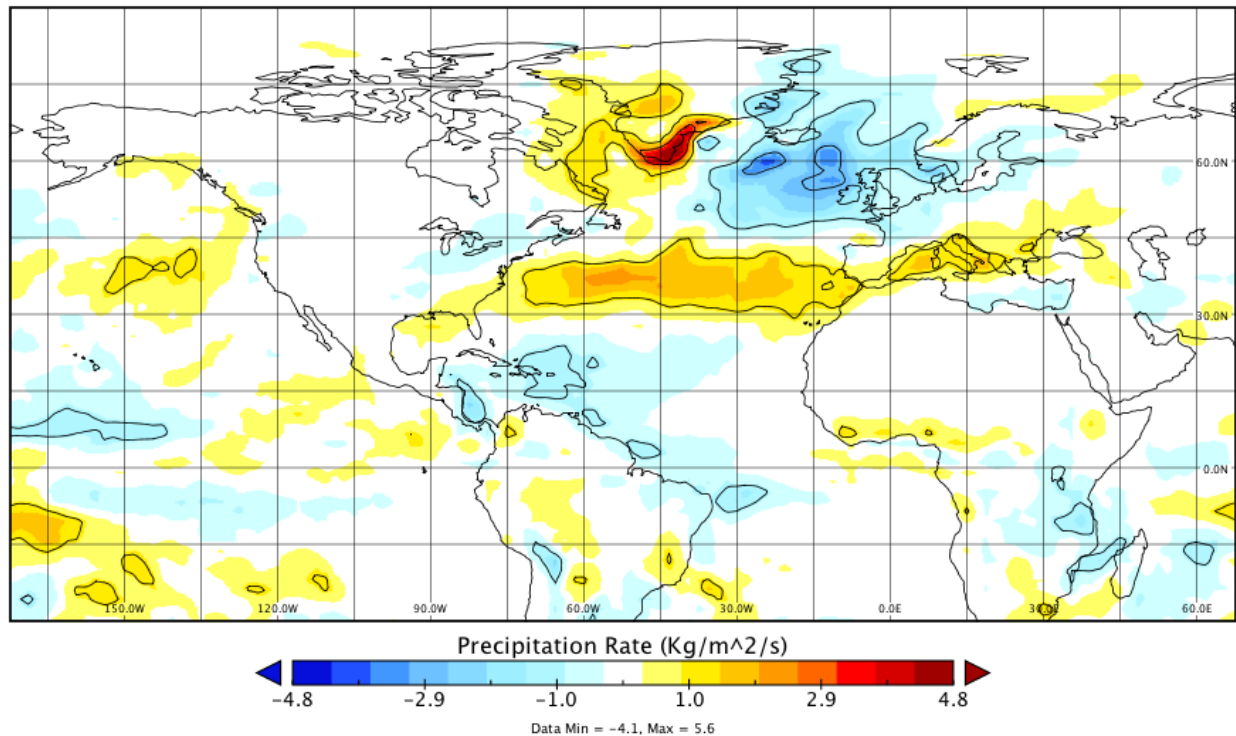


**Figure 9:** Composited precipitation rate anomalies for the duration of all 30 NA blocking events. Positive precipitation rates are present along the Atlantic storm track, displaced to the south by a strong blocking high near Iceland.

(meridional). Strong anti-cyclonic flow associated with the center of the blocking high is evident to the south of Greenland. A localized lull in wind speed just west of Ireland denotes the composite center of the NA blocking high. Three distinct jet streaks are recognizable in Figure 10 as well. A strong Pacific jet extends across much of the basin at 35°N and two additional jet maximums occur over the southeastern United States and north Africa respectively. The split jet stream configuration over the Atlantic and Africa is a common atmospheric response to strong winter time blocking in the North Atlantic (Li and Wettstein, 2012).

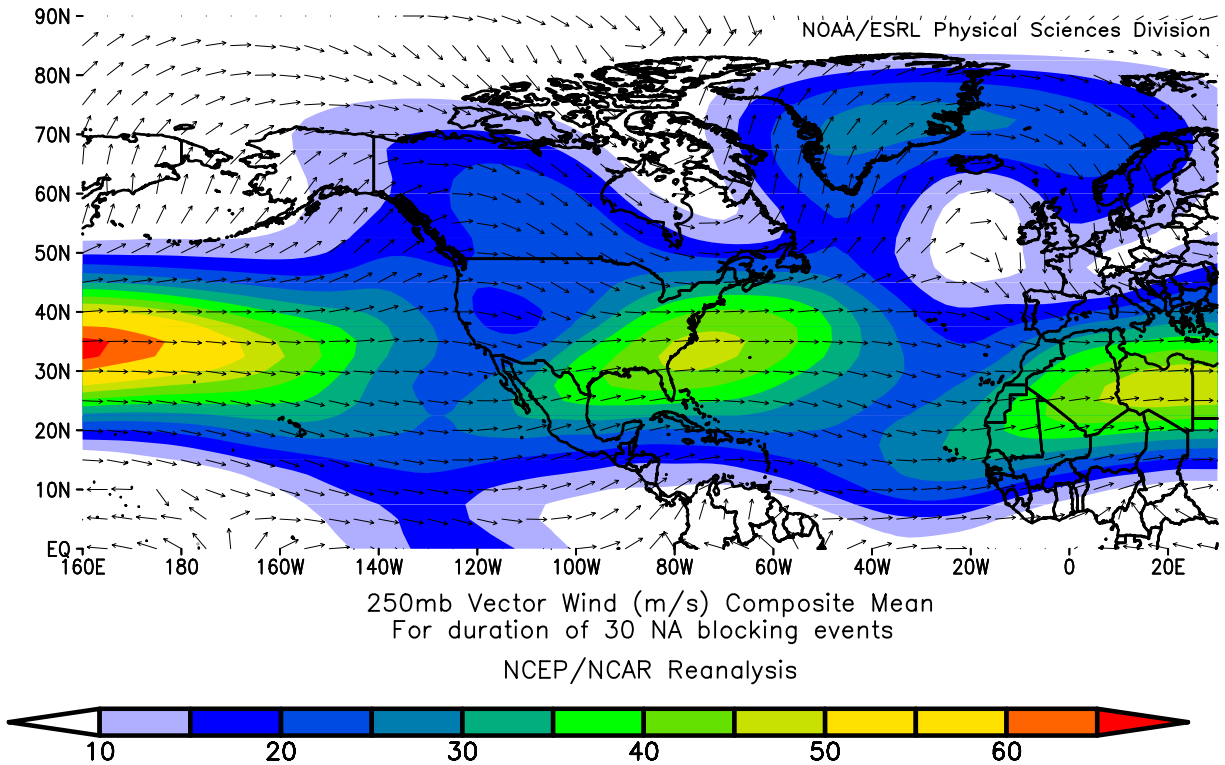


**Figure 10:** Composited mean vector wind (m/s) for the duration of all 30 NA blocking events. A split jet configuration is evident over the Atlantic basin, a response to the diverted westerly flow associated with the center of the blocking high just west of Ireland.

The jet maximum located over the southeastern U.S. is an eddy driven jet, split off from the subtropical jet located over north Africa. Eddy driven jets develop in areas of high baroclinicity (i.e.: a sharp meridional temperature gradient) and favor the formation of transient eddies, which were discussed as a blocking forcing mechanism in section 1.3.

Figure 11 displays the 250-hPa *u-wind* or zonal wind anomalies for the duration of the 30 NA blocking events. The zonal component of the vector wind is typically much larger than the meridional component and is a good estimation of jet stream location and strength. Two areas of maximum/minimum anomalies located over Greenland and south of Iceland represent flow anomalies as a result of the persistent anti-cyclonic flow centered around the blocking high.

Atlantic winter time blocking that occurs north of 45°N, closer to Greenland is too far displaced to completely inhibit typical westerly flow. As such, a common response to these events is the positive enhancement of zonal winds over the central Atlantic (Woolings, 2008). This can be seen in Figure 11 where a strong area of positive zonal anomalies exists at 30°N across the entire Atlantic basin.

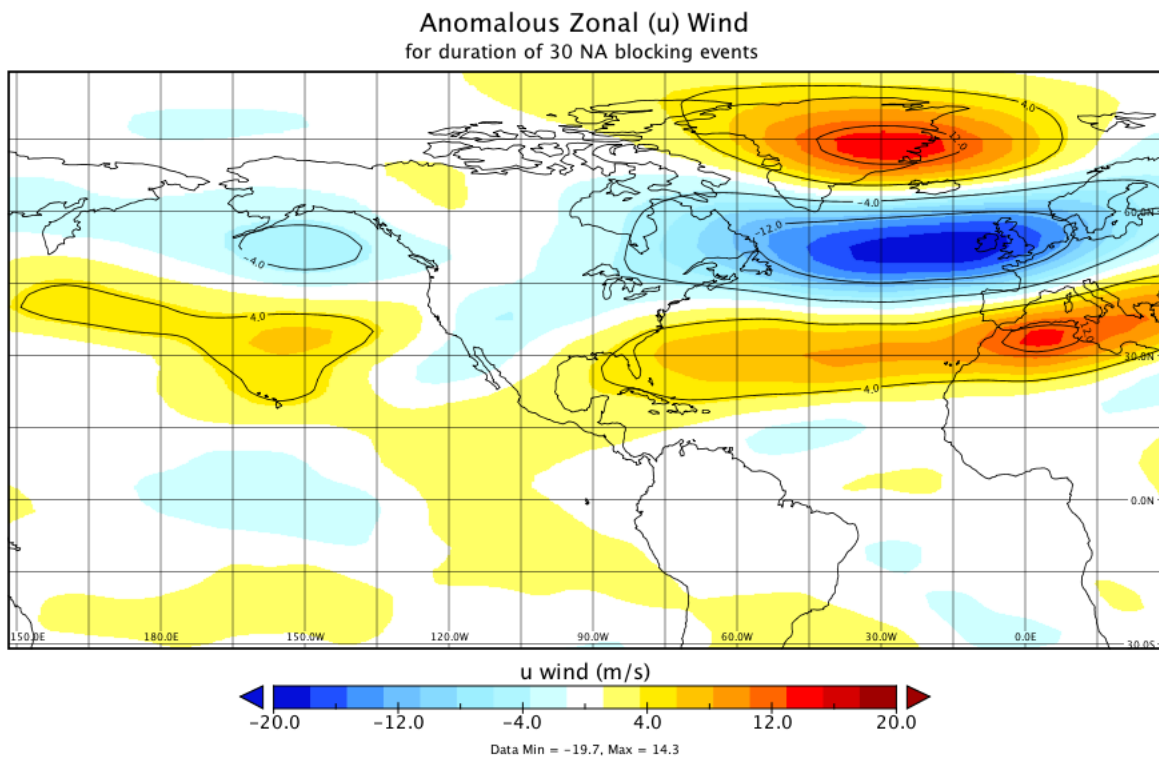


**Figure 11:** *Composited u-wind anomalies for the duration of all 30 NA blocking events. Anomalies associated with anti-cyclonic flow around the blocking high are evident in the North Atlantic. Positive anomalies over the Atlantic represent the storm track*

Figure 12 displays the 250-hPa *v-wind* or meridional wind anomalies for the duration of the 30 NA blocking events. Again, flow anomalies are evident with a strong positive anomaly exists on the western side of the NA blocking high while a strong negative anomaly is present on

the eastern side. The evolution of the meridional wind anomalies will serve as the central guide for precursor detecting.

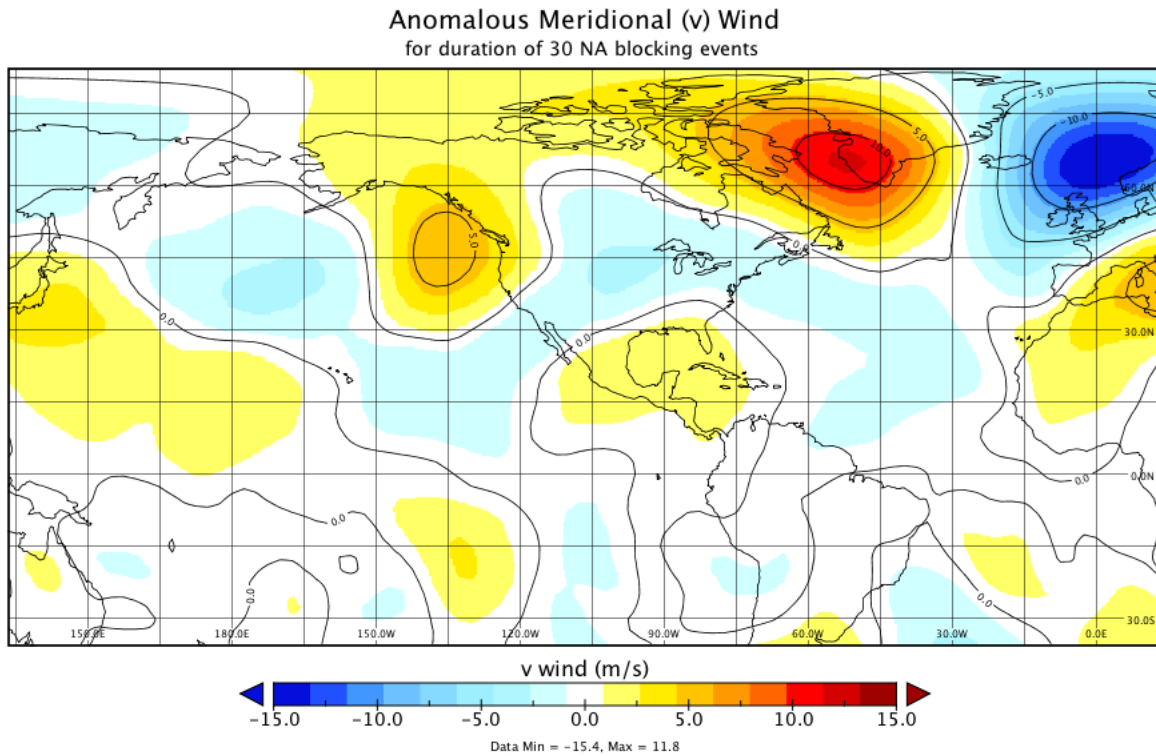


**Figure 12:** Composited  $v$ -wind anomalies for the duration of all 30 NA blocking events. Note the enhanced positive meridional signal over the southeastern U.S. in relation to the eddy stretching of rossby waves.

### 3.2 Lagged Composites and Evolution

A series of lagged time composites is presented to trace the evolution of NA blocking events and to ultimately identify precursor signals. These composites are presented in 5-day bulk averages, covering up to 3 weeks before the NA blocking event onset. As stated in section 2.1, the onset of a NA blocking event is defined as the date where all three blocking regime requirements are met.

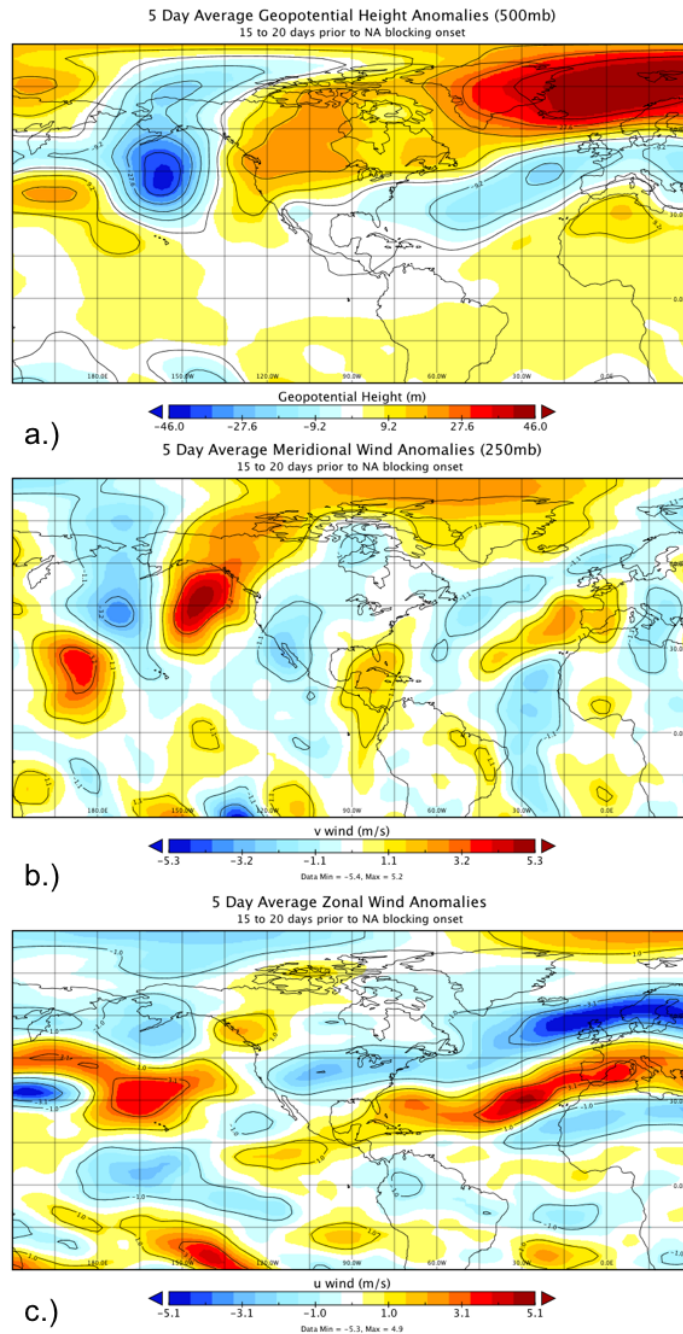
### ***3.2.1 Fifteen to twenty days prior to onset***

Figure 13 displays the 5-day average composited anomalies for the period 15 to 20 days before the NA blocking onset. Figure 13a shows a strong upper level low (Aleutian low) south of Alaska, while warm and positive height anomalies are evident over the central Pacific. A tightened pressure gradient develops on the southern edge of the Aleutian low close to the jet exit region. Increased baroclinicity in response to this configuration leads to westward expansion of the geopotential ridge of high pressure at the end of the storm track.

Further evidence of the ridge expansion can be seen in the meridional and zonal wind anomalies in Figure 13. The tightened pressure gradient at the southern edge of the Aleutian low results in enhanced positive zonal flow around 165°E in the central Pacific, which will serve to advect these warm anomalies eastward. Meanwhile, strong cyclonic flow results in positive meridional flow on the right side of the Aleutian low while strong anti-cyclonic flow on the left side of the western ridge also results in positive meridional flow.

### ***3.2.2 Ten to fifteen days prior to onset***

The westward expansion of the geopotential ridge results in enhanced meridional wind anomalies. Figure 14 illustrates the initiation of a meridional wave train of anomalies, known as a rossby wave train (Section 1.3). The eastward propagation (Figure 14b) of this rossby wave train serves as the main dynamical forcing behind the NA blocking events in the northern Atlantic and will be discussed in more detail in section 3.3. A series of positive and negative meridional wind anomalies located side by side with one another stretches from eastern Pacific all the way to the southeast U.S.



**Figure 13** 5-day average composites of a.) 500-hPa, b.) v-wind and c.) u-wind anomalies 15-20 days prior to the NA blocking onset. A tightened pressure gradient at the southern edge of the Aleutian low forces westward expansion of high pressure ridge.

The 500-hPa height anomalies in Figure 14a show a strong and expansive geopotential ridge located over the western United States. A storm track suppressed to the south is represented by a long and narrow band of negative height anomalies extending from the southwest U.S. all the way to western Europe. Two local minimums within this band are present off the off the southeastern U.S. coast and to the west of Portugal. These locations mark the exit region of the jet stream and areas of increased baroclinicity and storm development. The long band of positive zonal wind anomalies, co-located with the band of negative height anomalies, is another indication of a strong and suppressed storm track trough already present in this region.

Lastly, increased meridional flow over the southeastern United States, as a response to the rossby wave train, increases the meridional temperature gradient (baroclinicity) strengthening the geopotential trough already present in this region. This process was referred to as “preconditioning” the atmosphere in Colucci and Alberta (1996).

### ***3.2.3 Five to ten days prior to onset***

Figure 15a shows a much different 500-hPa pattern at 0.5 to 1.5 weeks prior to the NA blocking onset. The warm height anomalies from the central Pacific have migrated eastward, aiding the development of a deep low pressure trough that extends from the Gulf Coast of North America all the way into northern Canada. What’s left of the high-pressure ridge over the western part of the continent has been greatly reduced in size and scope.

Meanwhile, cyclogenesis over the southeastern United States is enhanced by the presence of a strong upper level low. Figure 15b highlights the enhanced positive meridional flow in the

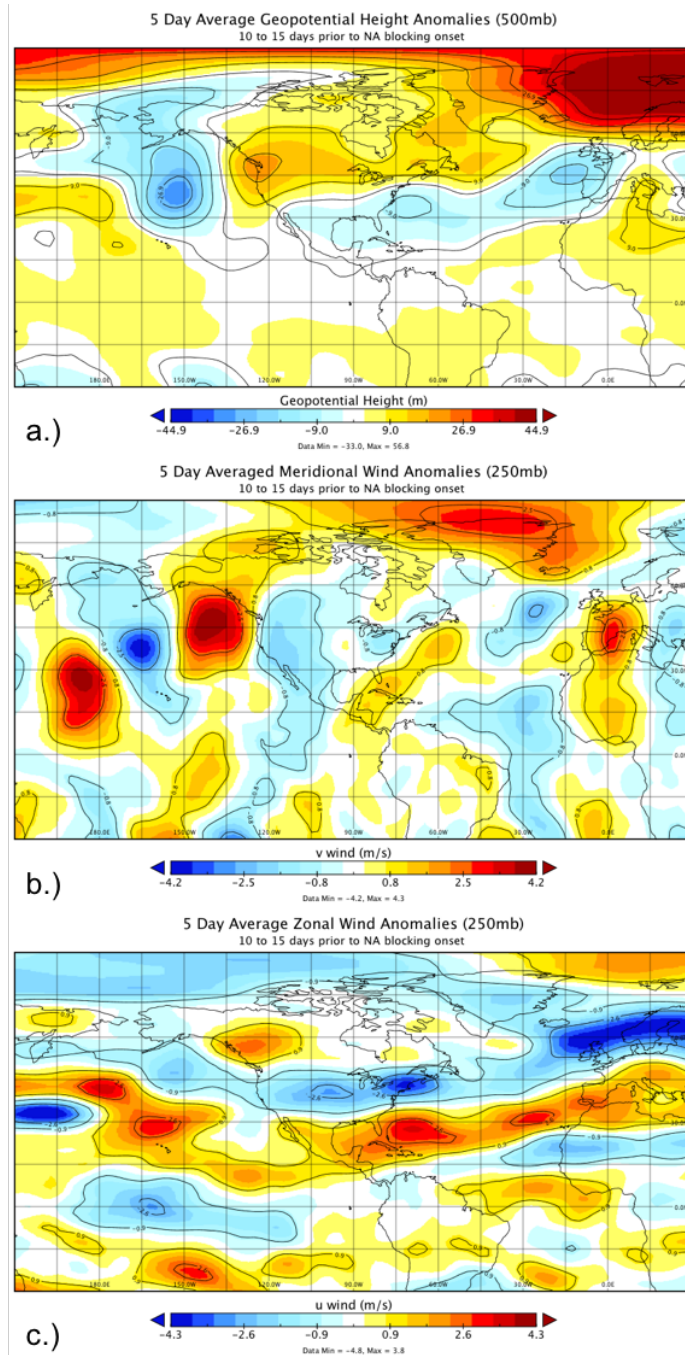


**Figure 14:** 5-day average composites of a.) 500-hPa; b.) v-wind and c.) u-wind anomalies 10-15 days prior to NA blocking event. The propagating of the rossby wave train from west to east is evident in the v-wind anomalies



same region, tightening the meridional temperature gradient and increasing baroclinicity. Therefore, favorable synoptic conditions (upper level low) combined with enhanced baroclinicity near a jet exit region adds up to an extremely complimentary environment for cyclogenesis.

Cyclone forward movement is impeded by a strong cold anomaly over the central Atlantic and a blocking high over central Europe. The slowdown in forward movement combined with the strong positive meridional anomalies stretches cyclones in the meridional direction. This process, referred to as eddy straining, will aid in the maintenance of the developing NA block. Additional evidence of a highly-amplified flow over the Atlantic is observed in Figure 15c, where a distinct dipole of positive/negative/positive *u*-wind anomalies exists across the entire basin.

#### ***3.2.4 Zero to five days prior to onset***

Figure 16 covers the 5-day averaged anomalies just before the onset of the NA blocking event. The 500-hPa anomalies show a strong blocking high in place just to the west of the key region. Figure 16a shows a highly-amplified flow over North America, with a deep low pressure trough over the western U.S. and a strong ridge of high pressure over the eastern U.S.

A split jet stream is visible in Figure 16c. The subtropical jet and its associated zonal flow is cut off from the jet stream over the Atlantic, separated by strong negative *u*-wind anomalies over the central Atlantic.

The meridional wind anomalies in Figure 16 b display a “wall” of highly positive anomalies, extending from the eastern U.S. all the way into Hudson Bay. This area represents eddy stretching of synoptic scale cyclones occurring for at least a week at this point. As

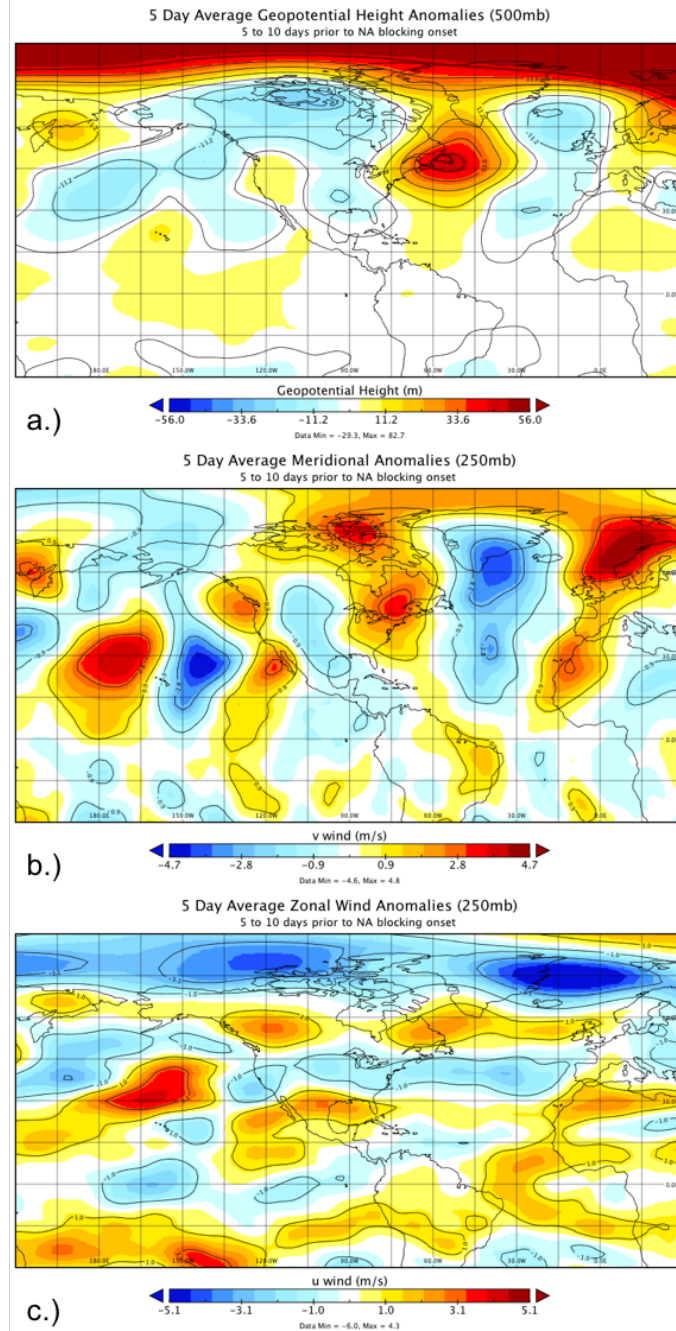


**Figure 15:** 5-day average composites of a.) 500-hPa; b.) v-wind and c.) u-wind anomalies 5-10 days prior to NA blocking event. Meridional eddy stretching over the U.S. east coast occurs because of low pressure trough blocking forward motion over central Atlantic.

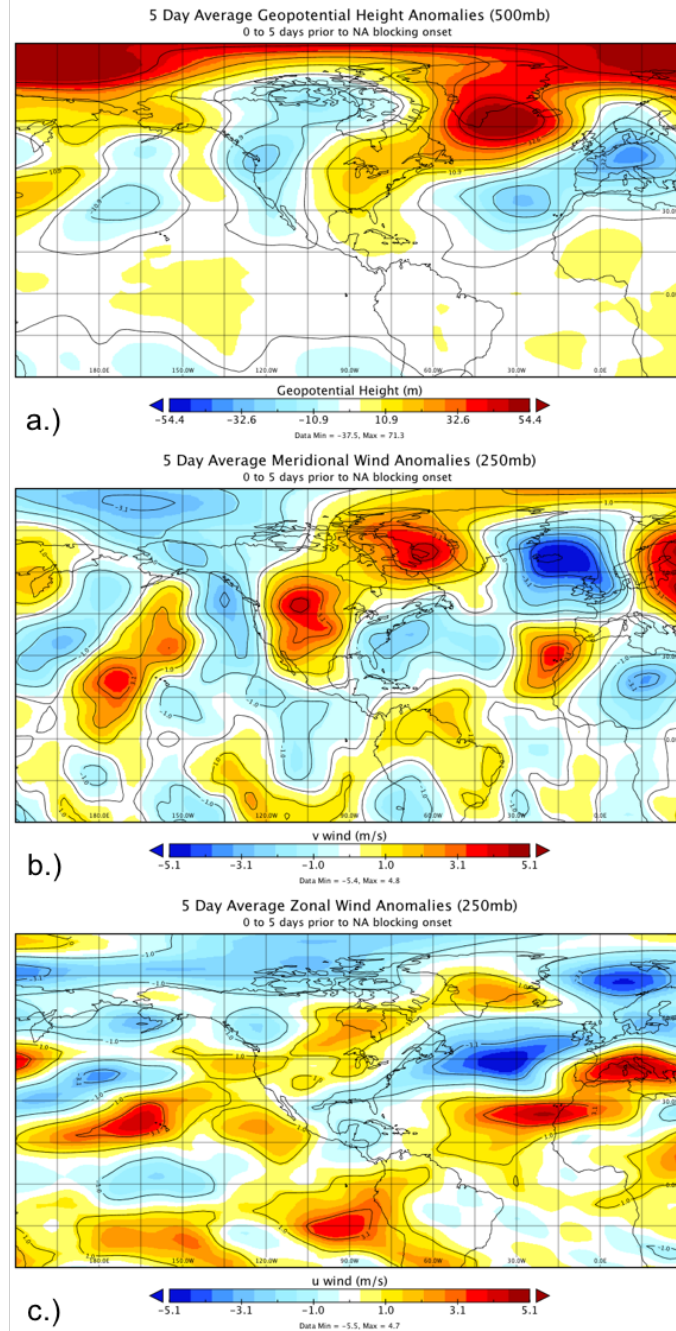


**Figure 16:** 5-day average composite of a.) 500mb; b.) v-wind; c.) u-wind anomalies 0-5 days prior to NA blocking event. Highly amplified, split jet flow develops in the presence of a strengthening blocking high over western Atlantic

mentioned in section 1.2.4 and depicted in Figure 3, the RWB associated with this configuration is the driving mechanism behind the persistence of NA blocking events.

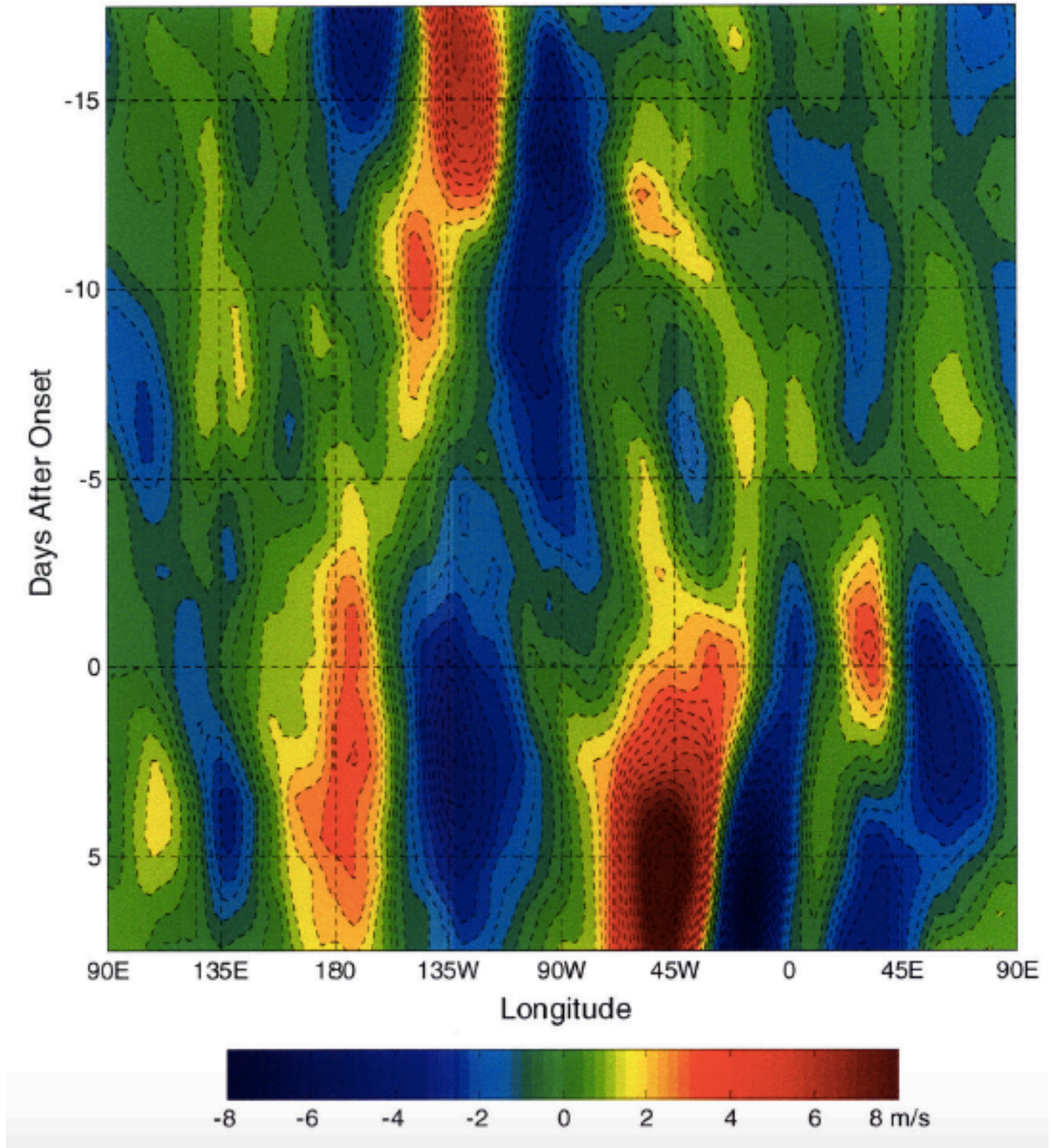
### **3.3 Hovmöller Diagram of Blocking Precursors**

Figure 17 displays the composited mid-latitude meridional wind anomalies leading up to the onset of the NA blocking event. The meridional wind anomalies in this figure display the anomalous meridional flow in both the Pacific and Atlantic Ocean basins. The presence of these anomalous winds up to 2 weeks before blocking onset represent a key precursor signal.

As described in Section 1, atmospheric blocking can be thought of as amplifying the climatological meridional flow both upstream and downstream of the block. This aspect of blocking is clearly seen in Figure 17, where the longitudinal region between 30°W and 80°W experiences an anomalous increase. Figure 17 shows clear evidence of a rossby wave train developing in the central Pacific 15 days prior to the NA blocking onset. This rossby wave train propagates to the east over the next two weeks, eventually becoming out of phase with the background mean flow. Further enhancement of the positive meridional signal ensues when the rossby wave train ultimately reaches the region of high baroclinicity over the southeastern U.S. (Figure 16b). The rossby waves become stretched meridionally, allowing the waves to break in a manner favorable to block maintenance.

### **3.4 NA Blocking and Teleconnections**

Teleconnection patterns are related to standing oscillations of planetary waves and can be used to further characterize global precursors to NA blocking events. Teleconnections are



**Figure 17** Hovmöller diagram of composite v-wind anomalies averaged between 40°N and 70°N, showing the precursor signal. Interval contours are 0.5 m/s

defined through strong correlations among either SLP or 500-hPa heights (Wallace and Gutzler,1981).

The three dominant teleconnection patterns in the Northern Hemisphere are the focus here. This includes the Pacific/North American pattern (PNA), the North Atlantic Oscillation (NAO) and the Arctic Oscillation (AO). The diagram below (Figure 18) displays the typical 500mb anomalies for one phase of each index.

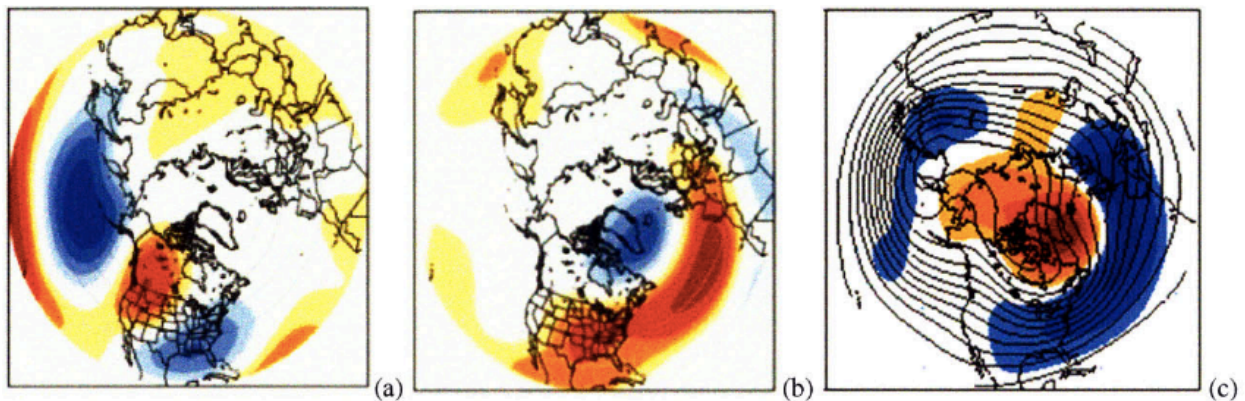


**Figure 18:** Winter time positive phase of the a.) PNA; b.) NAO and the c.) negative phase of the AO. Red(blue) shading indicates regions of warm (cold) 500-hPa anomalies. (Via Climate Prediction Center [http://www.cpc.noaa.gov/products/precip/CWlink/daily\\_ao\\_index/teleconnections.shtml](http://www.cpc.noaa.gov/products/precip/CWlink/daily_ao_index/teleconnections.shtml))

The PNA is comprised of four centers (Figure 18) with two upstream anomalies are located near Hawaii and the North Pacific, while two downstream anomalies are located over Alberta and the southeastern U.S. The positive PNA phase is characterized by a deep low pressure near the Aleutian Islands and a high-pressure ridge over the western U.S. The precursor signal established two weeks prior to NA blocking onset closely resembles a positive PNA pattern.

The typical 500-hPa anomalies for a positive PNA compared to the 500-hPa anomalies 10 to 15 days prior to the NA blocking onset are shown below (Figure 19). The four anomalous centers appear co located in both images. A composite time series of the PNA index for the 30

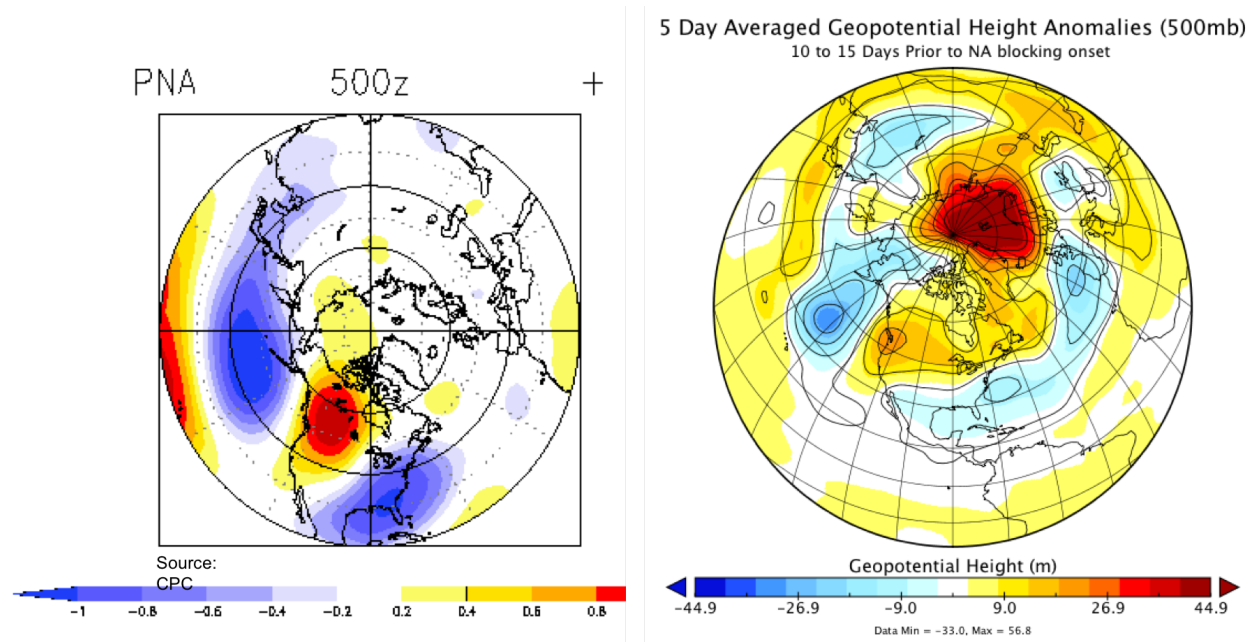


**Figure 19:** 500-hPa height anomalies associated with a positive PNA (left). 500-hPa height anomalies for the duration of the 30 NA blocking events (right).

NA blocking events (Figure 20) shows a distinct peak in the positive PNA phase nearly two weeks prior to the blocking onset.

The NAO is considered the leading variability pattern during the Northern Hemisphere winter (Barriopedro et al., 2006) and is made up of anomaly centers over the central Atlantic and Greenland. Several studies have shown that winter time blocking in the North Atlantic correlates with a negative NAO phase (Crocini-Masopli et al. 2007; Benedict et al. 2008). The composited

NAO index (Figure 20) shows a strong positive NAO phase leading up to the blocking onset followed by a sharp transition to a negative phase during the blocking event.

Studies have recently shown the importance of the AO in Northern Hemisphere weather variability (Wallace, 2000). The AO is associated with two anomaly centers with one over the polar regions and the other in the mid-latitudes. The NAO and AO are highly correlated; however, the NAO lacks a center of action in the Pacific. The composited AO index (Figure 20) shows that the AO index trends significantly negative before and during the NA blocking event. The sharp decline in the AO leads the negative trend in the NAO by several days, indicating the importance of global processes in establishing the NA block.

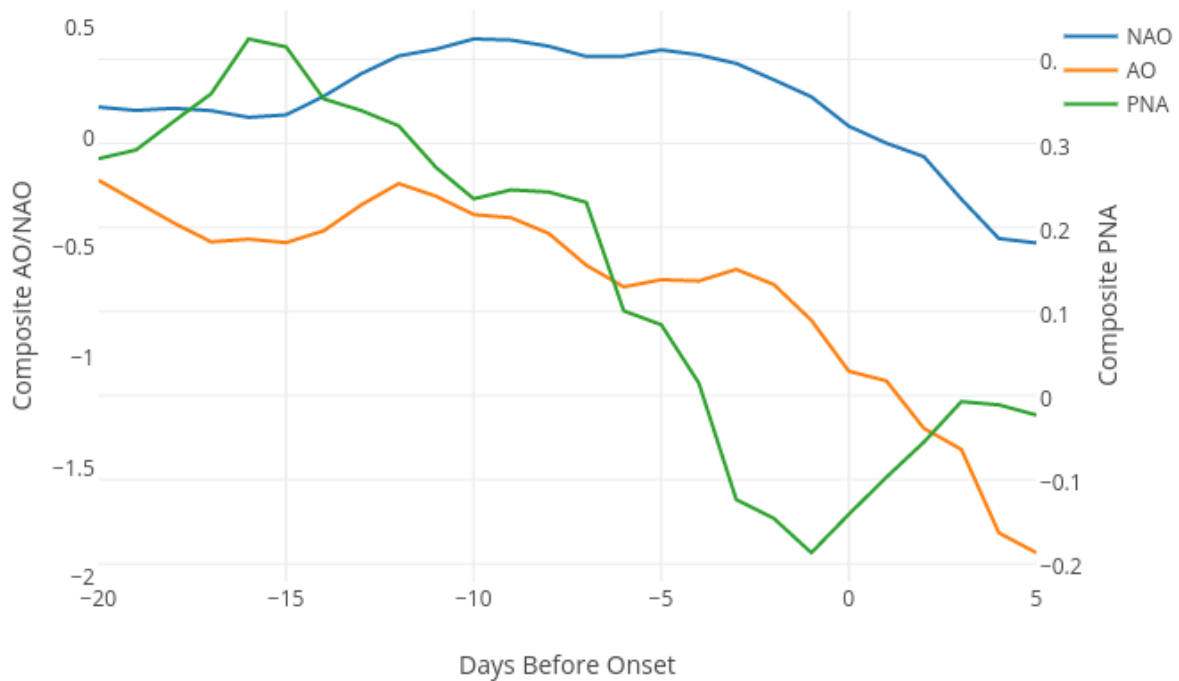


**Figure 20:** Composited PNA, NAO and AO indices for the duration of the 30 NA blocking events. A key precursor signal is found at 15 days prior to blocking onset, where the positive PNA index spikes, followed by a sharp fall off. Both the NAO and AO indices also trend negative leading up the blocking event, with the AO leading the NAO by several days.



## Chapter 4: Summary and Future Work

This study isolated strong and persistent winter blocking events in a specific region of the North Atlantic over the past 37 years. Composite analysis of 500-hPa height, *u-wind* and *v-wind* anomalies and associated atmospheric flow anomalies were used to track the evolution of these events. This analysis clearly identified several dynamical precursors leading up to these blocking events.

Approximately 15 to 20 days prior to the onset of the NA blocking event, warm height anomalies over the Central Pacific result in a tight pressure gradient on the southern edge of upper level (Aleutian) low in the same area as the jet exit region. Enhanced meridional flow around the tightened gradient becomes coupled with positive meridional flow on the eastern flank of the upper level low, invigorating the westward expansion of a high-pressure ridge centered over the western U.S.

At 10 to 15 days prior to onset and as a direct result of the ridge expansion, a distinctly positive PNA pattern peaks in the eastern Pacific. The circulation anomalies associated with this pattern kick starts a Rossby wave train, which propagates eastward and downstream.

After the peak positive PNA signal at 15 days prior to onset, the index begins a sharp negative transition over the next week. The phase transition corresponds to a pattern change over North America, with a breakdown of the pressure ridge over the western U.S and a strong upper level low over the southeastern U.S. As a result, increased cyclogenesis occurs near the southeast U.S.

Approximately 1 week before blocking onset, Atlantic cyclones forming over the southeastern U. S interact with the previously strong positive meridional signal created established by the rossby wave train, slowing forward motion and stretching the cyclones

meridionally. The stretching or eddy straining of these cyclones creates a short-wave environment that is out of phase with the background environment. As a result, the train of Rossby waves begin to break over the western Atlantic, ultimately promoting the genesis and maintenance of the NA blocking events.

Recent studies have shown that a positive PNA can be triggered by anomalous tropical convection in the western Pacific (Franzke et al. 2011). Additional research into tropical forcing and anomalous tropical convective activity could provide a more complete dynamical picture of the NA blocking precursor signal found in this study. The mature phase of NA blocking events strongly resembles the negative phases of two other main modes of atmospheric variability, the AO and NAO. The association of NA blocking events with simultaneous changes in several large-scale climate modes suggests that atmospheric blocking is indeed a global and not a local phenomenon.

Lastly, additional insight into precursor signals may be gained by utilizing a dynamic blocking index, such as the PV index proposed by Pelly and Hoskins (2003). Using such an approach would open the entire Atlantic basin for sampling as well as incorporate the important relationship between tropospheric and stratospheric interactions during blocking events.

## References

- Barriopedro, D., R. Garcia-Herrera, A. Lupo, and E. Hernandez, 2006: A Climatology of Northern Hemisphere Blocking. *Journal of Climate*, 19, 1042-1063
- Benedict, J., S. Lee, and S. Feldstein, 2004: Synoptic View of the North Atlantic Oscillation. *Journal of the Atmospheric Science*, 61, 121-144
- Berggren, R., B. Bolin, and C. Rossby, 1949: An Aerological Study of Zonal Motion, Its Perturbations and Break-down. *Tellus*, 1, 14-37
- Black, R.X and K. J. Evans, 1998: The Statistics of Horizontal Structure of Anomalous Weather Regimes in the Community Climate Model. *Monthly Weather Review*, 126, 841–859
- Carrera ML, Higgins RW, Kousky VE, 2004: Downstream Weather Impacts Associated with Atmospheric Blocking Over the Northeast Pacific. *J Clim.*, 17, 4823–4839
- Cassou, C., 2008: Intraseasonal Interaction Between the Madden–Julian Oscillation and the North Atlantic Oscillation. *Nature*, 455, 523–527
- Colucci, S. and T. Alberta, 1996: Planetary-scale Climatology of Explosive Cyclogenesis and Blocking. *Mon. Wea. Rev.* 124, 2509-2520
- Croci-Maspoli, M., C. Schwierz, and H. C. Davies, 2007: Atmospheric blocking: space-time links to NAO and PNA. *Climate. Dynamics*, 29, 713-725
- Dole, and N. D. Gordon, 1983: Persistent Anomalies of the Extratropical Northern Hemisphere Wintertime Circulation: Geographical Distribution and Regional Persistence Characteristics. *Mon. Wea. Rev.*, 111, 1567–1586
- Elliott, R. and T. Smith, 1949: A Study of the Effects of Large Blocking Highs on the General Circulation in the Northern-Hemisphere Westerlies. *Journal of Meteorology*, 6, 67-85
- Ferranti, L., F. Molteni, and T. Palmer, 1994: Impact of Localized Tropical and Extratropical SST Anomalies in Ensembles of Seasonal GCM Integrations. *Quarterly Journal of the Royal Meteorological Society*, 120, 1613-1645
- Franzke, C., S. Lee, and S. Feldstein, 2004: Is the North Atlantic Oscillation a Breaking Wave? *J. Atmos. Sci.*, 61, 145-160
- Franzke, C., Feldstein, S. B. and Lee, S., 2011: Synoptic Analysis of the Pacific–North American Teleconnection Pattern. *Q.J.R. Meteorol. Soc.*, 137, 329–346
- Frederiksen, J., 1997: Adjoint Sensitivity and Finite-Time Normal Mode Disturbances During Blocking. *J. Atmos. Sci.*, 54, 1144-1165

- Green, J., 1977: The Weather During July 1976: Some Dynamical Considerations of the Drought. *Weather*, 32, 120-126
- Grose, W. and B. Hoskins, 1979: On the Influence of Orography on Large-Scale Atmospheric Flow. *J. Atmos. Sci.*, 36, 223-234
- Hansen, A. and T. Chen, 1982: A Spectral Energetics Analysis of Atmospheric Blocking. *Mon. Wea. Rev.*, 10, 1146-1165
- Held, I., M. Ting, and H. Wang, 2002: Northern Winter Stationary Waves: Theory and Modeling. *J Clim*, 15, 2125-2144
- Higgins, R.W., and S.D Schubert, 1996: Simulations of Persistent North Pacific Circulation Anomalies and Interhemispheric Teleconnections. *J. Atmos. Sci.*, 53, 188–207
- Hoskins, B., I. James, and G. White, 1983: The Shape, Propagation and Mean-Flow Interaction of Large-Scale Weather Systems. *J. Atmos. Sci.*, 40, 1595-1612
- Hoskins, B. and P. Sardeshmukh, 1987: A Diagnostic Study of the Dynamics of the Northern Hemisphere Winter of 1985-86. *Q. J. Roy. Meteorol. Soc.*, 113, 759-778
- Kalnay, E., et al., 1996: The NCEP/NCAR 40-Year Reanalysis Project. *Bull. Amer. Meteor. Soc.*, 77, 437–471
- Egger, J., 1978: Dynamics of Blocking Highs. *J Atmos. Sci.*, 35, 1788-1801
- Li C, Wettstein JJ., 2012: Thermally Driven and Eddy-Driven Jet Variability in Reanalysis. *J. Clim.* 25: 1587–1596
- Namias, J., 1947: Characteristics of the General Circulation Over the Northern Hemisphere During the Abnormal Winter 1946-47. *Mon. Wea. Rev.*, 75, 145-152
- Nakamura, H., M. Nakamura, and J. Anderson, 1997: The Role of High- and Low-Frequency Dynamics in Blocking Formation. *Mon. Wea. Rev.*, 125, 2074-2093
- Pelly, J. L., and B. J. Hoskins, 2003a: A New Perspective on Blocking. *J. Atmos. Sci.*, 60, 743–755
- Renwick, J. A., 1998: ENSO-Related Variability in the Frequency of South Pacific Blocking. *Mon. Wea. Rev.*, 126, 3117–3123
- Rex, D., 1950a: Blocking Action in the Middle Troposphere and its Effect Upon Regional Climate: I. An aerological study of blocking action. *Tellus*, 2, 196-211
- Rex, D., 1950b: Blocking Action in the Middle Troposphere and its Effect Upon Regional Climate, *Tellus*, 2, 275–301

- Rossby, C., 1950: On the Dynamics of Certain Types of Blocking waves. *Journal Chinese Geophysical Society*, 2, 1-13
- Schwierz C, Croci-Maspoli M, Davies HC., 2004: Perspicacious Indicators of Atmospheric Blocking. *Geophys Res Lett.*, 31,6125–6128
- Shutts, G., 1983: The Propagation of Eddies in Diffluent Jet Streams: Eddy Vorticity Forcing of Blocking Flow Fields. *Q. J. Roy. Meteorol. Soc.*, 109, 737-761
- Sillmann, J., M. Croci-Maspoli, M. Kallache, and R. W. Katz, 2011: Extreme Cold Winter Temperatures in Europe under the Influence of North Atlantic Atmospheric Blocking. *J Clim.*, 24, 5899-5913
- Simmons, A., J. Wallace, and G. Branstator, 1983: Barotropic Wave Propagation and Instability, and Atmospheric Teleconnection Patterns. *J. Atmos. Sci.*, 40, 1363-1392
- Nigam,S and E. DeWeaver, 2003: Stationary Waves (Orographically and Thermally forced). *Encyclopedia of Atmospheric Sciences*; Editors: J.R. Holton, J.A. Pyle, and J.A. Curry; Academic Press, Elsevier Science, London, 2121-2137
- Sumner, E., 1954: A Study of Blocking in the Atlantic-European of the Northern Hemisphere. *Q. J. Roy. Meteorol. Soc.*, 80, 402-416
- Tibaldi, S. and F. Molteni, 1990: On the Operational Predictability of Blocking. *Tellus*, 42A, 343-365
- Trigo, R., I. Trigo, C. DaCamara, and T. Osborn, 2004: Climate Impact of the European Winter Blocking Episodes from the NCEP/NCAR Reanalysis. *Climate Dynamics*, 23, 17-28
- Tsou, C. and P. Smith, 1990: The Role of Synoptic/Planetary Scale Interactions During the Development of a Blocking Anticyclone. *Tellus A*, 42, 174-193
- Tung, K. and R. Lindzen, 1979: A Theory of Stationary Long Waves. Part I: A Simple Theory of Blocking. *Mon. Wea. Rev.*, 107, 714-734
- Tyrlis, E. and B. Hoskins, 2008: The Morphology of Northern Hemisphere Blocking. *J. Atmos. Sci.*, 65, 1653-1665
- Wallace, J. M., and D. S. Gutzler, 1981: Teleconnections in the Geopotential Height Field During the Northern Hemisphere Winter. *Mon. Wea. Rev.*, 109, 784-812
- Woollings, T., B. Hoskins, M. Blackburn, and P. Berrisford, 2008: A New Rossby Wave Breaking Interpretation of the North Atlantic Oscillation. *Journal of Atmospheric Science*, 65, 609-326

Woollings, T., 2008: Vertical Structure of Anthropogenic Zonal-Mean Atmospheric Circulation Change. *Geophys. Res. Lett.*, 35, L19 702.

Woollings, T., A. Hannachi, and B. Hoskins., 2010: Variability of the North Atlantic Eddy-Driven Jet Stream, *Q. J. Roy. Meteorol. Soc.*, 136, 856–868

## Supplemental Figures

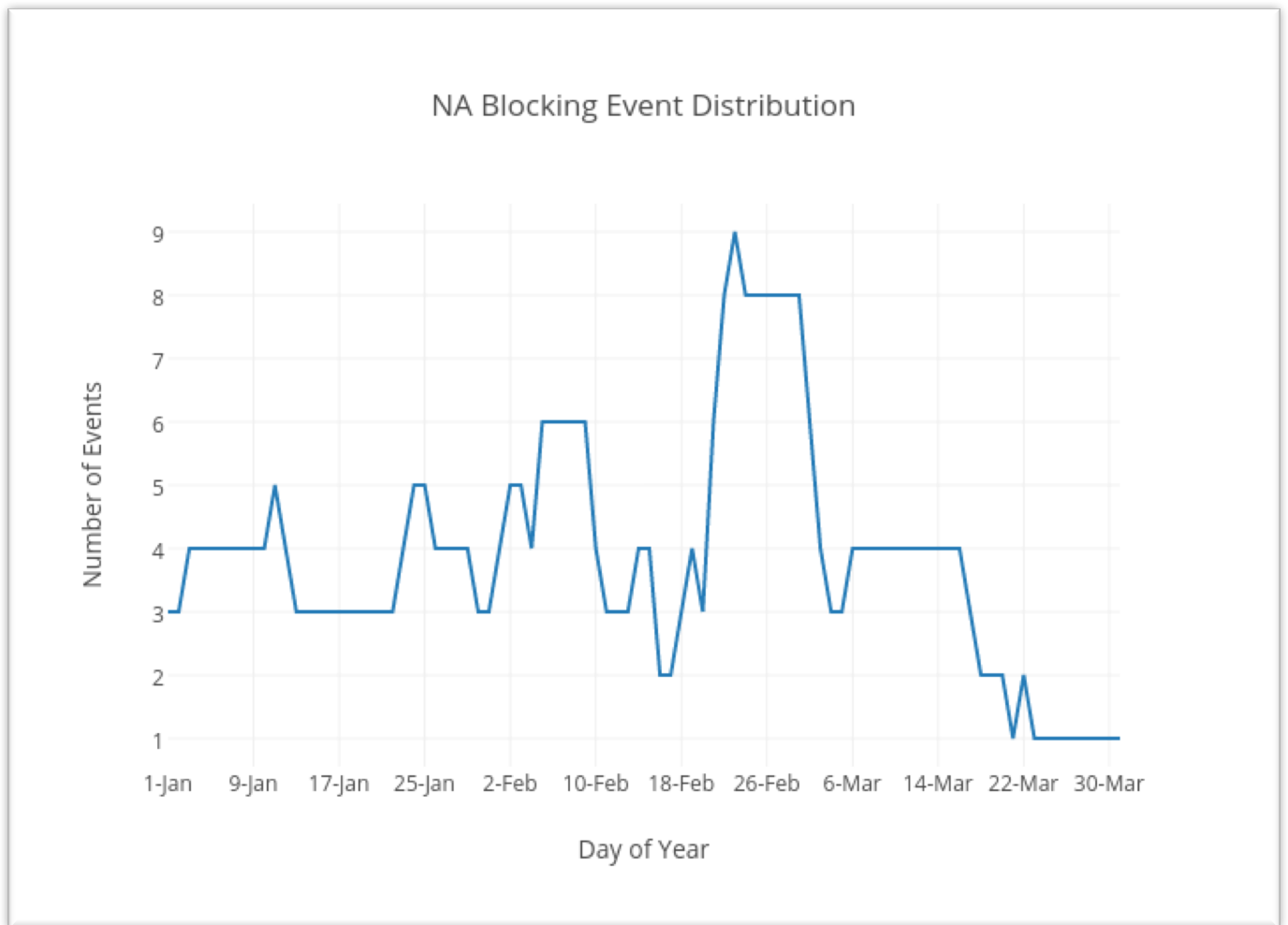


**Figure 21:** Daily distribution of the 30 NA blocking events

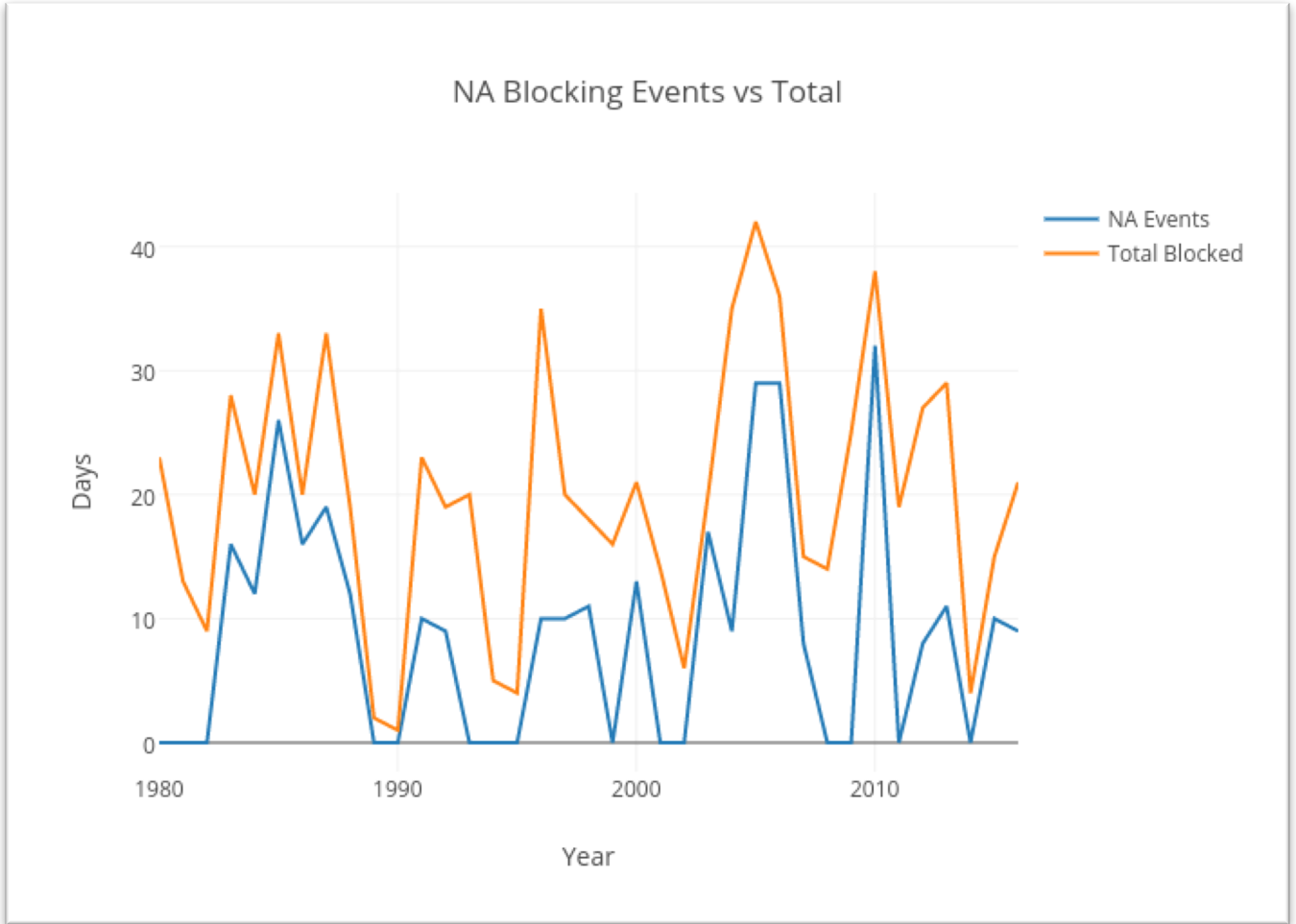


*Figure 22: NA blocking days vs. total blocked days*

Climatology of Geopotential Heights  
for Jan-Mar 1980-2016

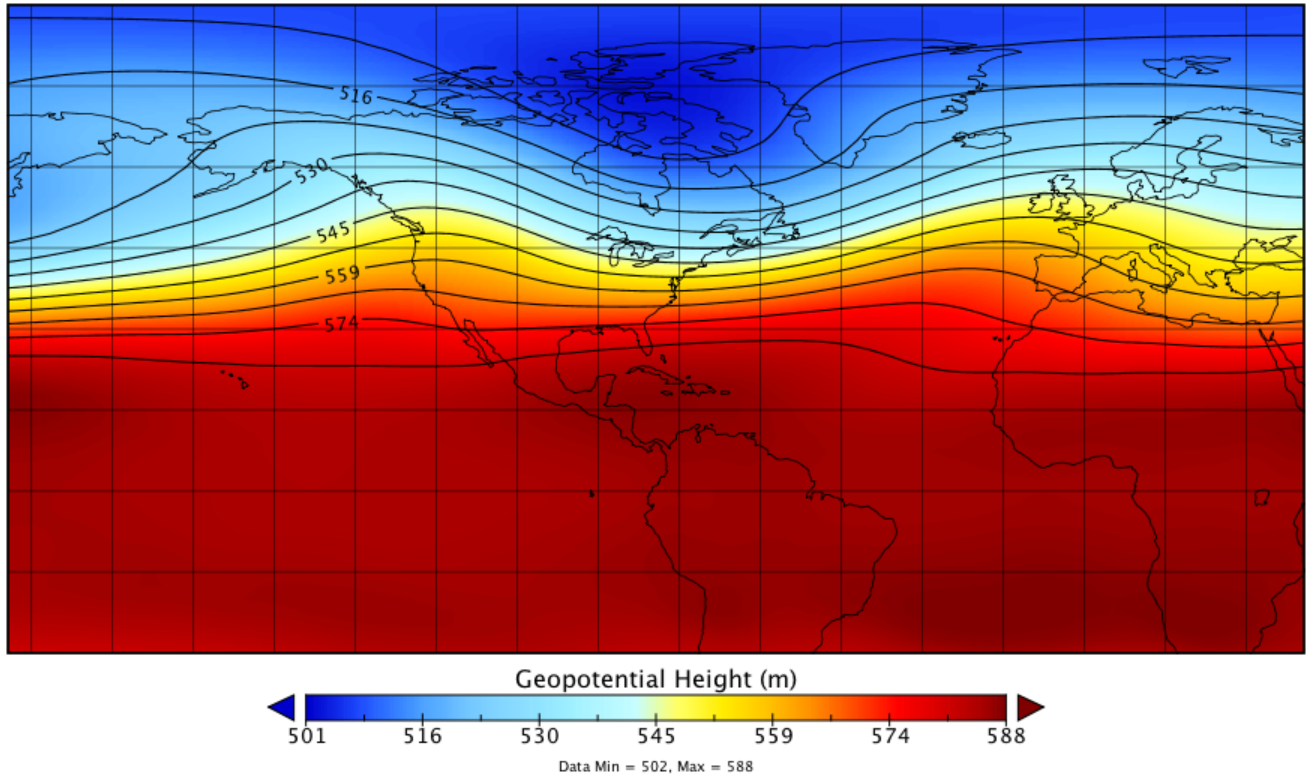


*Figure 23: Climatology of winter time 500-hPa heights from 1980-2016*



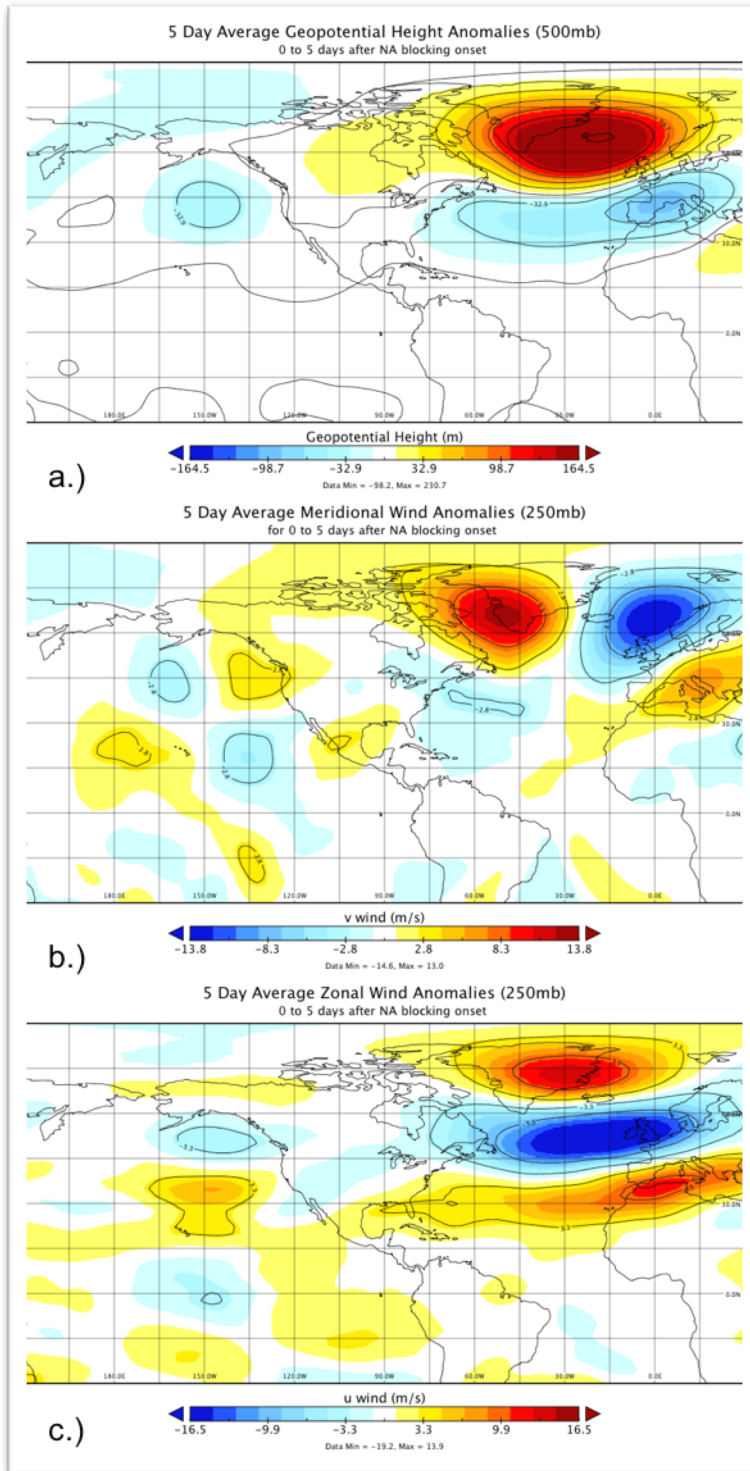


*Figure 24: 5-day composite anomalies of a.) 500-hPa height; b.) v-wind; c.) u-wind 0 to 5 days after NA blocking onset*

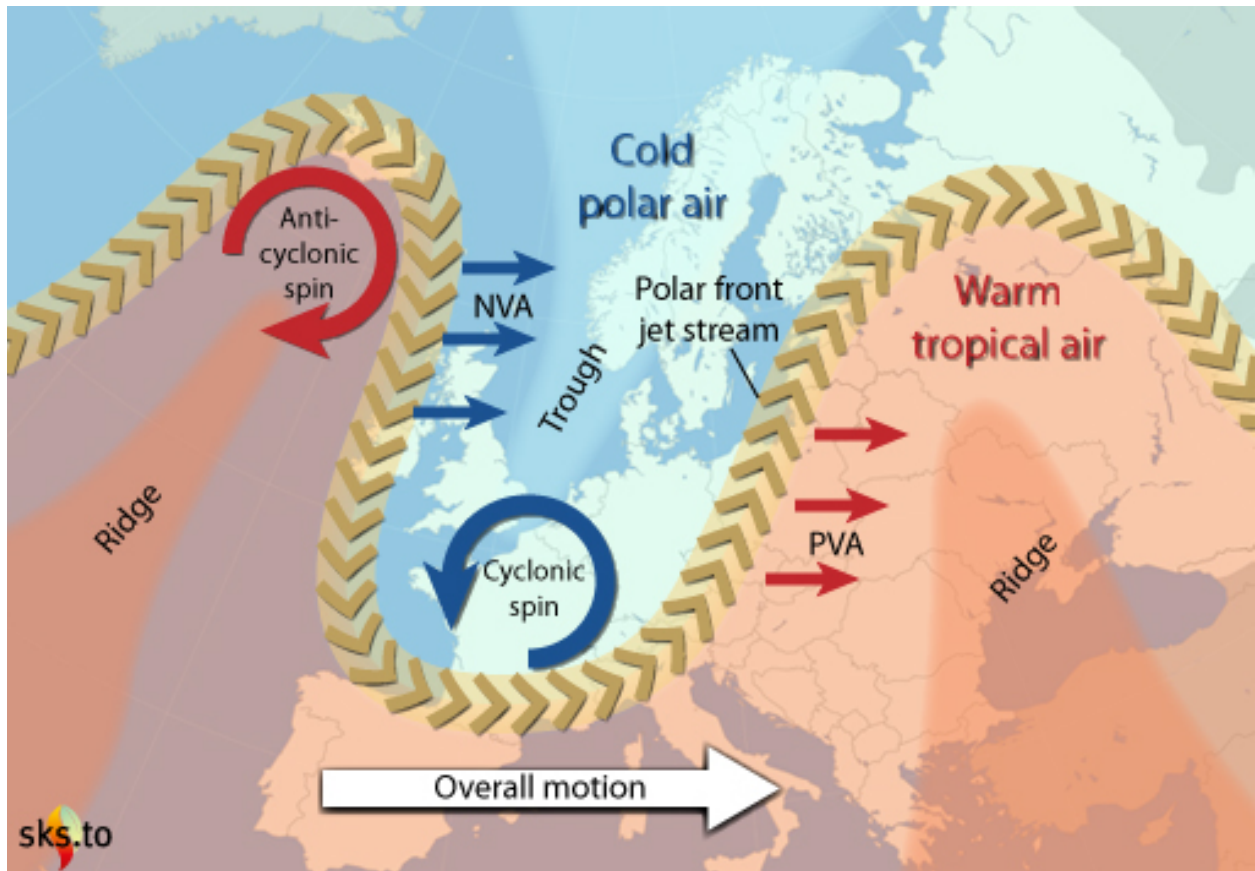


*Figure 25: Diagram depicting the resulting flow anomalies in an amplified (highly kinetic) jet stream pattern.*

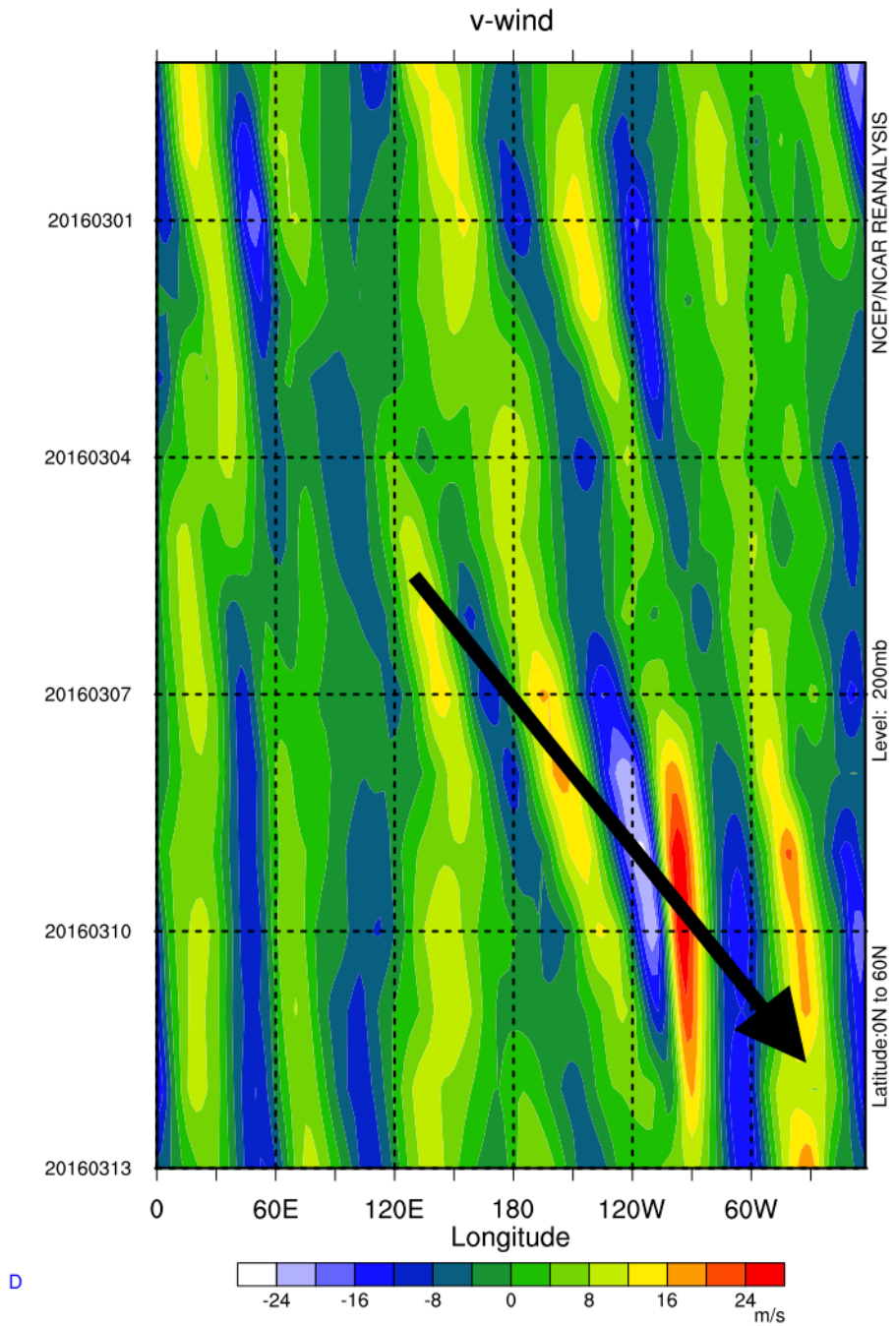


*Figure 23: Rossby wave train propagation from NA case number 30. The black arrow highlights the negative/positive anomalous meridional signal associated with a rossby wave train*